



1 **Impacts of a large flood along a mountain river basin: unravelling the geomorphic**  
2 **response and large wood budget in the upper Emme River (Switzerland)**

3

4 Virginia Ruiz-Villanueva<sup>1</sup>, Alexandre Badoux<sup>2</sup>, Dieter Rickenmann<sup>2</sup>, Martin Böckli<sup>2</sup>, Salome Schläfli<sup>3</sup>, Nicolas  
5 Steeb<sup>2</sup>, Markus Stoffel<sup>1,4,5</sup>, Christian Rickli<sup>2</sup>

6

7 <sup>1</sup>Institute for Environmental Sciences, University of Geneva, Boulevard Carl-Vogt 66, 1205 Geneva, Switzerland

8 <sup>2</sup>Swiss Federal Research Institute WSL, Zürcherstrasse 111, CH-8903 Birmensdorf, Switzerland

9 <sup>3</sup>Institute of Geological Sciences, University of Bern, Baltzerstrasse 1+3, 3012, Bern, Switzerland

10 <sup>4</sup>Department of Earth Sciences, University of Geneva, 13 rue des Maraîchers, 1205 Geneva, Switzerland

11 <sup>5</sup>Department F.-A. Forel for Aquatic and Environmental Sciences, University of Geneva, 66 Boulevard Carl  
12 Vogt, 1205 Geneva, Switzerland

13

14 *Correspondence to:* Virginia Ruiz-Villanueva (Virginia.Ruiz@unige.ch)

15



16 **Abstract**

17 On July 24, 2014, an exceptionally large flood (recurrence interval ca. 150 years) caused large-scale inundations,  
18 severe overbank sedimentation and damage to infrastructures and buildings along the Emme river (central  
19 Switzerland). Widespread lateral bank erosion occurred along the river, thereby entraining sediment and large  
20 wood (LW) from alluvial forest stands. This work analyses the catchment response to the flood in terms of  
21 channel widening and LW recruitment and deposition, but also identifies the factors controlling these processes.  
22 We found that hydraulic forces (e.g., stream power index) or geomorphic variables (e.g., channel width, gradient,  
23 valley confinement), if considered alone, are not sufficient to explain the flood response. Instead, spatial  
24 variability of channel widening was firstly driven by precipitation, and secondary by geomorphic variables (e.g.,  
25 channel width, gradient, confinement and forest length). LW recruitment was mainly caused by channel widening  
26 (lateral bank erosion) and thus also controlled by precipitation. In contrast, LW deposition was controlled by  
27 channel morphology (mainly channel gradient and width). However, we also observed that extending the analysis  
28 to the whole upper catchment of the Emme river, including all the tributaries and not only to the most affected  
29 zones, resulted in a different set of significant explanatory or correlated variables. Our findings highlight the need  
30 to continue documenting and analysing channel response after floods at different locations and scales. Whereas  
31 this is key for a better process understanding, the identification of controlling factors can also contribute to the  
32 identification of critical reaches, which in turn is crucial for the forecasting and design of sound river basin  
33 management strategies.

34

35

36 **Keywords:** large flood, channel changes, channel widening, large wood, woody debris.

37



## 38 **1 Introduction**

39 Floods in mountain river basins are characterized by complex, yet extreme meteorological events and  
40 subsequent, equally complex process coupling between the hillslopes and channels (i.e., debris flows, debris  
41 floods, and floods), resulting in a high spatial variability of morphological responses (Harvey, 1986; Miller,  
42 1990; Lapointe et al., 1998; Magilligan et al., 1998; Heritage et al., 2004; Arnaud-Fassetta, 2013; Savi et al.,  
43 2013; Thompson and Croke, 2013, Rickenmann et al., 2016). During high intensity events, mass-movement  
44 processes (e.g., landslides, debris flows) may affect channel morphology and sediment supply, influencing the  
45 total sediment load during a flood (Lin et al. 2008). In forested areas, mass movements and bank erosion do not  
46 only deliver large amounts of inorganic sediment, but also introduce large quantities of wood into the channel  
47 corridor. As a load component in forested rivers, large wood (defined as wood pieces exceeding 10 cm in  
48 diameter and 1 m in length; LW) can be placed in a similar framework to that used for sediment, where LW  
49 recruitment, transport, and deposition are the main processes to be understood a part of the LW budgeting  
50 (Gurnell, 2007). The presence of wood in rivers has very positive effects in general (Ruiz-Villanueva et al., 2016  
51 and references within); however, LW and sediment in channels can also favour the creation of temporary dams  
52 and subsequently produce secondary flood pulses, thereby enhancing erosion, and/or leading to the destruction of  
53 infrastructure along the channel (Cenderelli and Kite 1998; Wohl et al., 2010; Ruiz-Villanueva et al., 2014).  
54 Flood damage and flood losses are intrinsic to the occurrence of major floods (Merritts, 2011). However,  
55 urbanization, an increase in impervious surfaces (Hollis, 1975) and river channelization or embankment  
56 constructions (Wyżga, 1997) are frequently invoked as well to explain the high economic losses caused by major  
57 flood events (Hajdukiewicz et al., 2015). Under such conditions, even frequent floods (i.e., lower magnitude  
58 events) can lead to unexpectedly high damage.

59 Over the last decades, several major flood events occurred in different parts of Switzerland (e.g., August  
60 1978, August 1987, September 1993, May 1999, October 2000, August 2005, and August 2007; Hilker et al.,  
61 2009; Badoux et al., 2014), thereby causing significant financial damage costs. The August 2005 flood was by far  
62 the costliest natural disaster in Switzerland since the start of systematic records in 1972 (Hilker et al., 2009),  
63 claimed six lives and caused a total financial damage costs exceeding three billion Swiss Francs. The dominant  
64 processes observed during this event were flooding, bank erosion, overbank sedimentation, landslides, and debris  
65 flows (Rickenmann and Koschni, 2010; Rickenmann et al., 2016). Moreover, the transport and deposition of  
66 more than 69,000 m<sup>3</sup> of LW along alpine and pre-alpine rivers has been recorded (Steeb et al., 2017; Rickli et al.,



67 2018). The consequences of events like the one in 2005 pose threats to important infrastructure such as roads and  
68 settlements and therefore, these processes need to be better understood and quantified to provide a valuable  
69 process understanding and improved preparedness.

70 However, predicting the impacts of major floods on the fluvial system is very challenging and requires a  
71 wide range of analyses (Rinaldi et al., 2016; Surian et al., 2016). Some of the most recent studies in the field  
72 focused on the (i) reconstruction of the hydrological event (e.g., Gaume et al., 2004); (ii) analysis of flood  
73 hydraulic variables (e.g., Howard and Dolan, 1981; Miller, 1990; Wohl et al., 1994; Benito, 1997; Heritage et al.,  
74 2004; Thompson and Croke, 2013); (iii) hillslope processes and channel connectivity (e.g., Bracken et al., 2015  
75 and 2013; Croke et al., 2013; Wohl, 2017); (iv) geomorphic and sedimentological analysis of flood deposits (e.g.,  
76 Wells and Harvey, 1987; Macklin et al., 1992); (v) quantification of morphological changes (e.g., Arnaud-  
77 Fassetta et al., 2005; Krapesch et al., 2011; Thompson and Croke, 2013; Comiti et al., 2016; Surian et al., 2016;  
78 Righini et al., 2017); (vi) sediment budgeting (e.g., Milan, 2012; Thompson and Croke, 2013); or (vii) more  
79 recently, the study of LW dynamics and budgeting (e.g., Lucía et al., 2015; Steeb et al., 2017).

80 Post-event surveys are invaluable when it comes to improve insights on flood related processes (Gaume  
81 and Borga, 2008; Marchi et al., 2009; Rinaldi et al., 2016) such as LW recruitment and factors controlling LW  
82 deposition, which are both crucial for a proper management of river basins and flood hazard mitigation (Comiti et  
83 al., 2016). Despite this fact, analyses of LW dynamics after flood events remain quite rare (Comiti et al., 2016).  
84 In this study, we added this important component to the post-event survey after the July 2014 flood in the Emme  
85 river. The specific aim thereby was to provide a quantitative description of several coupled processes (i.e., debris  
86 flows, landslides, bank erosion, and/or flooding) and the geomorphic effects of this major event (mainly in terms  
87 of channel widening). We paid attention to morphological changes, the coupling between hillslopes and  
88 headwaters to the main channel, the supply of large quantities of LW and its deposition through the river corridor.  
89 We extended the analysis to the whole upper catchment of the Emme river, including all tributaries, and not only  
90 the ones that were most affected in July 2014. By doing so we aimed at unravelling diverging responses among  
91 the different tributaries and river segments in terms of geomorphic changes and LW dynamics. The hypothesis  
92 was that in terms of morphology, similar river sub-reaches may have responded differently to the flood. As river  
93 reach response is driven by several parameters, we selected different morphological and hydrometeorological  
94 variables to identify the factors controlling channel widening, LW recruitment, and LW deposition.

95



## 96 **2 Material and methods**

### 97 **2.1 The Emme river basin**

98 The Emme River takes its origin in the Swiss Prealps (1400 m a.s.l.) and runs through the Emmental, in the  
99 Cantons of Luzern and Bern in central Switzerland. Total drainage area at its mouth with the Aare River (near the  
100 city of Solothurn) is 963 km<sup>2</sup>, with a stream length of 80 km.

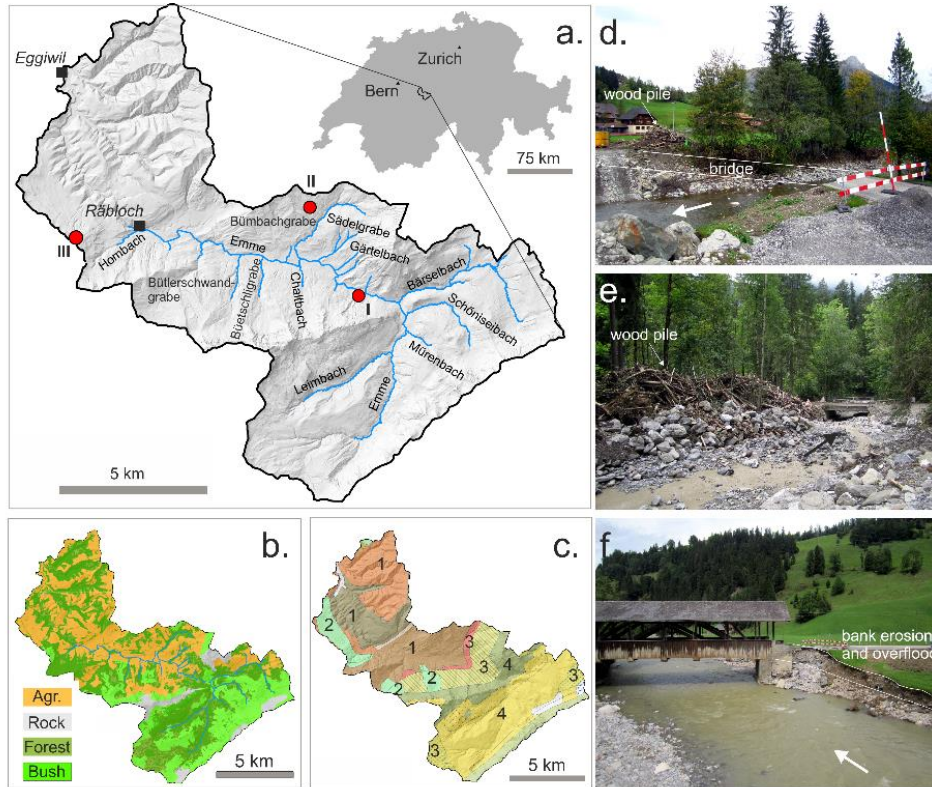
101 Geology of the basin is composed mainly by Helvetic marginal limestone, the Ultrahelvetian flysch (with  
102 marls and sandstones) and sub-alpine molasse composed of sandstone, molasse conglomerates and marls  
103 (Lehmann, 2001). During the Pleistocene glaciation, a large part of the Emmental was covered by glaciers and  
104 moraines remains are preserved in the areas of Eggiwil, Oberburg or Burgdorf.

105 The Emme basin is extensively occupied by agricultural lands (50%, mostly downstream), 40% of the  
106 surface remains forested today, and only about 10% is urbanized. Climate is temperate with moderate warm  
107 summers (mean temperature in July is 16°C according to the Langnau data series from 1931-2015; Federal Office  
108 of Meteorology and Climatology MeteoSwiss) and cold winters (mean temperature -1°C in January). Total annual  
109 precipitation averaged 1315 mm at the station of Langnau (1901-2015), with mean monthly peaks in June of 160  
110 mm. The flow regime of the Emme River is characterized by a seasonally fluctuating flow due to snowmelt in  
111 spring and thunderstorms in summer.

112 This work focuses on the Upper Emme River basin (Figure 1), including the uppermost tributaries to the  
113 inlet of the Emme River into a gorge called Räßloch. At this point, the Emme river basin has a drainage area of  
114 94 km<sup>2</sup> and the network is formed by 19 streams (18 tributaries and the main branch of the Emme; Table 1).  
115 These 19 streams were further divided into 64 sub-reaches as explained in the Methods (see also Figure S1 in the  
116 supplementary material).

117 A history of severe flooding has led to intensive river management activities in the 19<sup>th</sup> and 20<sup>th</sup> centuries  
118 with the construction of dams and weirs. These measures also resulted in an isolation of tributaries and low  
119 sediment transport (Figure S2). Additionally, poor riparian conditions and water extractions for irrigation  
120 strongly influenced Emme River hydrology (Burkhardt-Holm and Scheurer, 2007).

121 Figure 1 shows an enlarged basin up to the only existing stream gauge in the area (Eggiwil station located  
122 at 745 m a.s.l. and with a drainage area of 124 km<sup>2</sup>), which is several kilometres downstream of the Räßloch  
123 gorge.



124

125 *Figure 1: Location of the basin in central Switzerland (a) Hill shade of the Upper Emme River basin (up to*  
 126 *Eggiwil), red dots show the location of the rain gauges (I: Kemmeriboden; II: Marbachegg; III:*  
 127 *Schallenberg), blue lines show the 19 streams analysed (18 tributaries and the main river Emme); (b)*  
 128 *Land use: Agr.: Agriculture; Rock: Bare soil; Forest; Bush: Shrubs and bushes; (c) Geology: 1*  
 129 *Quaternary and Neogene molasses; 2 Moraines; 3 Paleogene Flysch; 4 Cretaceous and Jurassic*  
 130 *sedimentary rocks; (d) Debris flow and LW deposits in the lower part of the Sadelgrabe torrent upstream*  
 131 *its confluence with the Emme river (photograph: V. Ruiz-Villanueva); (e) Road and bridge washed away*  
 132 *during the flood in Bumbach (photograph: V. Ruiz-Villanueva); (f) Räbeli bridge damaged during the*  
 133 *flood (photograph: V. Ruiz-Villanueva). Arrows show the flow direction.*

134



135 *Table 1: Overview of the 19 study streams, sub-reaches in each stream and number of transects analysed,*  
 136 *morphological characteristics (Av.: averaged or total values) and total maximum and mean precipitation*  
 137 *registered during the event in 2014 at each sub-catchment (explained in the text).*  
 138

Stream name	Sub-reaches	Total N° of transects	Drainage Area (km <sup>2</sup> )	Total stream length (m)	Total forested channel length (m)	Av. stream Gradient	Av. Width before (m)	Av. Width ratio	Av. Sinuosity	Total max. Precip. (mm)	Total mean precip. (mm)
Bärselbach	12, 14, 15, 17, 18, 21, 23, 26, 27	127	13.1	7017	6276	0.048	7	1.74	1.27	92	69
Buembachgrabe	42, 43	86	4.9	4553	3913	0.062	10	1.48	1.14	97	86
Büetschligrabe	50, 51	17	2.3	1000	841	0.051	5	1.00	2.54	65	46
Bütlerschwandgrabe	53	28	2.8	1580	1248	0.137	11	1.01	1.21	62	46
Chaltbach	45	10	1.5	563	493	0.090	4	1.07	1.37	70	48
Emme	3, 4, 7, 11, 28, 30, 33, 36, 37, 40, 41, 44, 46, 48, 49, 52, 54, 55, 58, 59, 61, 62, 63	352	93.7	20571	12361	0.023	15	1.40	1.36	97	87
Gärtelbach	38	39	0.7	1769	1769	0.185	5	3.11	1.07	94	91
Hombach	64	19	2.8	922	907	0.082	8	1.48	1.37	50	38
Leimbach	1, 2	80	9.2	4402	4167	0.054	6	1.35	1.27	49	36
Sädelgrabe	39	79	1.6	3434	3219	0.123	6	4.75	1.25	97	94
Schöniseibach	8, 9, 10	28	4.5	1476	1280	0.085	7	1.06	1.27	81	65
Schwarzbach	56, 57	13	5.4	768	768	0.080	7	1.18	1.28	59	41
Stream	16, 22, 24, 25, 31, 32	37	1.0	1915	1787	0.133	5	1.82	1.30	92	89
Stream (Gerbehüsi)	60	3	0.2	227	227	0.193	6	1.00	1.25	53	48
Stream (Kemmeriboden)	29	12	0.3	610	610	0.256	5	3.11	1.09	92	67
Stream (Kemmerli)	34, 35	13	0.5	647	564	0.142	5	2.42	1.15	93	90
Stream (Schneeberg)	19, 20	16	1.1	846	751	0.099	6	1.57	1.34	87	79
Stream (Unterlochseite)	47	12	1.2	607	79	0.073	3	2.08	1.31	76	71
Mürenbach	5, 6	12	2.4	650	650	0.092	5	0.99	1.47	67	52

139

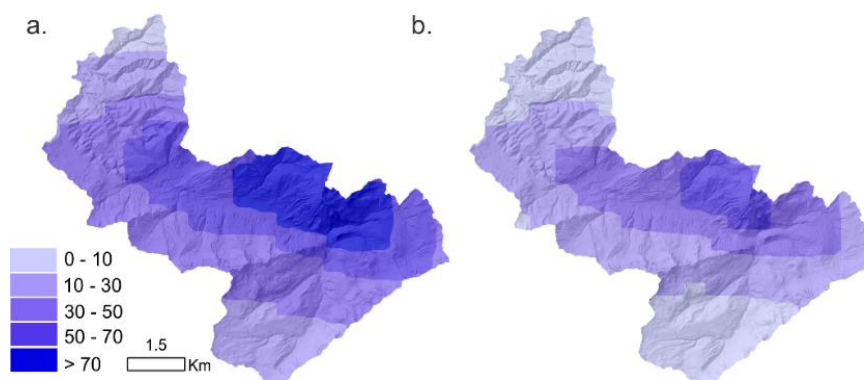
140

## 141 **2.2 The July 24, 2014 flood event**

142 July 2014 was a very wet month in Switzerland with frequent and extensive rainfall in the first three  
 143 weeks, interrupted by a few dry intervals. Data of MeteoSwiss showed that the western half of Switzerland  
 144 registered twice to three times the long-time precipitation average for the month of July 2014 (FOEN, 2015).  
 145 These wet episodes have led to saturated soils, especially in the western and northeastern parts of Switzerland  
 146 (FOEN, 2015; ARGE LLE Schangnau-Eggiwil, 2015). Between 24 and 28 July 2014, several thunderstorms



147 occurred over different Swiss regions. Until 27 July, the storms were related to a weak pressure system over  
148 Western Europe (MeteoSwiss, 2017). Generally, such relatively uniform pressure distributions result in light and  
149 variable winds at ground level which allows for the formation of cumulonimbus clouds, typically over regions  
150 with rough topography such as, e.g., the Swiss Prealps. On 24 July, an extremely violent stationary thunderstorm  
151 developed with a precipitation hotspot located over the upper Emmental. The storm cell caused intense rainfall in  
152 the headwater catchments of the upper Emme basin where it triggered very severe floods. According to hourly  
153 CombiPrecip data of MeteoSwiss (Sideris et al., 2014), the heavy precipitation yielded maximal hourly values of  
154 approximately 65 mm locally (with totals reaching 96 mm during the 7-hour event; Figure 2). Heavy rainfall was  
155 largely restricted to the upper Emme catchment with a local maximum just north of the Sädelgraben catchment.  
156 The cantonal rain gauge Marbachegg (red dot II in Figure 1) that recorded the highest event precipitation value of  
157 76 mm is located roughly two kilometres northwest of the confluence of the Sädelgraben torrent with the Emme  
158 river. According to ARGE LLE Schangnau-Eggiwil (2015) the rainfall event was associated to a recurrence  
159 interval between 100 and 200 years.



160

161 *Figure 2: Map of the spatial distribution of the precipitation (mm) on the 24 July 2014 in the Upper Emme*  
162 *catchment: (A) Total event precipitation (mm) from 04:00 to 17:00h; (B) maximum hourly precipitation*  
163 *recorded at 07:00 AM.*

164

165 Due to the wet soil conditions caused by all the antecedent rain, several of the small steep tributaries of the  
166 Emme river reacted very quickly to the 24 July 2014 rainstorm.

167 The receiving Emme river produced an exceptionally large flood. The discharge station in Eggiwil (124  
168 km<sup>2</sup> catchment area, 38 years of records) registered a peak discharge of 338 m<sup>3</sup> s<sup>-1</sup> which corresponding to a  
169 recurrence interval of ~150 years (FOEN, 2017). Runoff in Eggiwil rose very quickly and reached a maximum





170 within only a few hours. In the framework of the local post-event analysis, peak values of the Emme runoff  
171 upstream of the gauging station Eggiwil were estimated for this flood based on downstream measurements and by  
172 using local flood marks (ARGE LLE Schangnau-Eggiwil, 2015; Table 2).

173

174 *Table 2: Peak discharges along the Emme during the 24 July 2014 flood, measured or estimated in the*  
175 *framework of the local event analysis for several sites along the Emme river (data source: ARGE LLE*  
176 *Schangnau-Eggiwil, 2015). Note that the drainage area given here does not precisely correspond to data*  
177 *in Table 2 because estimates were carried out where flood marks were available.*

Point along the Emme	Drainage area (km <sup>2</sup> )	Peak discharge (best estimate) (m <sup>3</sup> s <sup>-1</sup> )	Range of peak value (m <sup>3</sup> s <sup>-1</sup> )
Kemmeriboden	51	240	204-276
Bumbach	67	300	255-345
Schangnau	86	330	281-380
Räbloch	94	280*	238-336
Eggiwil (Heidbüel)	124	338	Stream gauge record

178 \* *the reduction in discharge at these two sections is due to the clogging of the Räbloch gorge and related*  
179 *backwater effects.*

180

181 Hydrographs were reconstructed for Schangnau and Räbloch (ARGE LLE Schangnau-Eggiwil, 2015).  
182 Peak discharge amounted to approximately 240 m<sup>3</sup> s<sup>-1</sup> at Kemmeriboden (51 km<sup>2</sup> catchment area). Along our  
183 study reach, peak values probably increased until Schangnau where they reached about 330 m<sup>3</sup>·s<sup>-1</sup>. In a natural  
184 gorge between the villages of Schangnau and Eggiwil (a place called Räbloch; 94 km<sup>2</sup> catchment area), the  
185 Emme river was impounded due to clogging. A temporary lake formed and according to field surveys peak runoff  
186 was reduced to about 280 m<sup>3</sup> s<sup>-1</sup> (ARGE LLE Schangnau-Eggiwil, 2015).

187 At the Eggiwil gauging station, a first slight increase in discharge was recorded just after 06:00 AM and  
188 runoff reached 50 m<sup>3</sup>·s<sup>-1</sup> (a discharge statistically reached during one day per year based on data from 1975-2016)  
189 at approximately 09:00 AM. Five and a half hours later, at 02:30 PM, the runoff along the falling limb of the  
190 Emme hydrograph decreased below 50 m<sup>3</sup>·s<sup>-1</sup>. Peak discharge at Eggiwil was reached at approximately 10:30  
191 AM, about half an hour after the peak occurred at Räbloch. Hence, the 24 July 2014 flood event in the Emme was  
192 short. Similarly, short floods with a very steep rising hydrograph limb took place in June 1997 (245 m<sup>3</sup>·s<sup>-1</sup>) and  
193 July 2012 (178 m<sup>3</sup>·s<sup>-1</sup>), both caused by very intensive convective rain storms as well. Further major floods that  
194 occurred in the 42 years of measurement were registered in 2005 and 2007 (both with peaks slightly above 175  
195 m<sup>3</sup>·s<sup>-1</sup>). However, these events were much longer due to the long-lasting nature of the triggering precipitation  
196 event (Bezzola and Hegg, 2007; Bezzola and Ruf, 2009).



197 The Emme River overflowed at various points in the upper catchment and caused large-scale inundations  
198 and severe overbank sedimentation (Figure 1). Infrastructure, flood protection structures as well as buildings  
199 were damaged, and in some cases, even destroyed. Moreover, widespread bank erosion occurred all along the  
200 Emme River, thereby entraining sediments and wood from alluvial forest stands.

201 The steep torrents produced considerable debris floods and debris flows and transported large amounts of  
202 sediment and LW. The two most active torrents (Sädelgraben and Gärtlebach) overtopped their channels and  
203 deposited ample amounts of material on their fans. Near the confluence of the Sädelgraben and the Emme River,  
204 the road was obstructed by several meters of coarse material from the torrents. Furthermore, shallow landslides  
205 and hillslope debris flows occurred on steep locations of the upper Emme catchment.

206 The lower part of the Gärtelbach (from an elevation around 1300 m a.s.l.) delivered around 2000 m<sup>3</sup> of sediment  
207 to the Emme river, most of it recruited in the fluvial corridor, with 5000–7000 m<sup>3</sup> sediment deposited on the fan.  
208 The other main sediment source into the Emme river was the Sädelgrabe, where around 2000 m<sup>3</sup> of sediment was  
209 deposited in the channel, and around 15,000 m<sup>3</sup> of sediment deposited on the cone (according to ARGE LLE  
210 Schangnau-Eggiwil, 2015). However, sediment budgeting or deeper analysis about sediment dynamics was out  
211 the scope of our work.

212 Financial damage to private property and infrastructure (e.g., roads, bridges, hydraulic structures) in the  
213 worst affected municipalities of Schangnau and Eggwil was estimated at approximately 20 million Swiss Francs  
214 (Andres et al., 2015).

215

216

## 217 **2.3 Methods**

### 218 *2.3.1. Field survey*

219 A post event survey was carried out right after the flood and during the following weeks. The Swiss  
220 Federal Office for the Environment (FOEN) initiated a project to study the recruitment, transport, and deposition  
221 of large wood in the upper catchment of the Emme River (Badoux et al., 2015; Böckli et al., 2016; Rickli et al.,  
222 2016), in which the main geomorphic effects of the flood were analysed as well (Zurbrügg, 2015). This project  
223 was elaborated in close collaboration with the local authorities (ARGE LLE Schangnau-Eggiwil, 2015).

224 The field survey after the flood focused on the quantification of deposited wood, identification of  
225 recruitment sources, and identification of changes in planform geometry (i.e., bank erosion). The field survey was



226 carried out along 9.5 km of the Emme River and two of its main tributaries (Sädelgrabe and Gärtelbach),  
227 although other tributaries were visited as well. Regarding large wood, source areas (including landslides or debris  
228 floods and bank erosion) were identified in the field and mapped in GIS, and wood deposits were measured.  
229 Moreover, we noted whether LW from hillslopes processes reached the streams, as most of the mass movements  
230 were shallow landslides and not directly connected to the channel network.

231 Each piece of LW (length > 1m and diameter > 10 cm; Wohl et al., 2010) deposited during the flood along  
232 the studied reaches was assigned to a class relative to its mid-length diameter and length (Marcus et al., 2002;  
233 Daniels, 2006; Lucía et al., 2015; Rickli et al., 2016), i.e., seven classes were distinguished from < 10 cm to > 40  
234 cm in diameter and nine classes from < 2 to > 16 m for length. Log volume was calculated as solid cylinders  
235 (Thévenet et al., 1998). Wood accumulations were also measured. The wood volume of each jam was calculated  
236 geometrically through its area and height (measured in the field), considering a 50–80% range in porosity  
237 (Thévenet et al., 1998).

238 In the tributary catchments where large quantities of wood were deposited, mainly along the Sädelgrabe  
239 fan, the extension of wood deposits and size of accumulations prevented the measurement of individual pieces.  
240 Areas with similar density of wood were identified and plots were measured to estimate total wood volume in the  
241 area (see Figure S3). Most of the recruited wood from the Gärtelbach was deposited along the Emme floodplain.

242 Civil protection services removed some of the wood deposits immediately after the flood, storing the  
243 material at two sites close to the river, one near the confluence between the Sädelgrabe and the Emme and  
244 another near the Bumbach bridge (Figure 1). These piles (five in total) were analysed as well and wood samples  
245 were measured to estimate the stored wood volume and wood size distribution (Rickli et al., 2016).

246

247

### 248 2.3.2. GIS analysis

249 The field survey was complemented with GIS analyses with the aim to extend the study to the upper  
250 catchment and to include all tributaries. The entire upper catchment was analysed by splitting the stream network  
251 into 64 sub-reaches according to the tributaries junctions and the location of bridges, as bridges may act as  
252 obstacles to the downstream transfer of wood (see Figure S1). A total of 54.5 km of stream network length were  
253 analysed.

254 For all sub-reaches, we calculated key morphological and hydrological parameters, such as maximum and  
255 minimum elevation, channel gradient, channel sinuosity, or drainage area by using the available DEM for the



256 catchment (SwissALTI3D, 2 m spatial resolution) and spatial analysis and the hydrological geoprocessing. Other  
257 morphological parameters such as valley bottom width were extracted from the DEM using the Fluvial Corridor  
258 tool (Alber and Piégay, 2011; Roux et al., 2014). Moreover, the available aerial orthoimages (Swisstopo) were  
259 used to map the active channel before (image from March 2014, resolution 25 cm) and after (image from May  
260 2015, resolution 25 cm) the flood. The post flood units were mapped as well in the field, with a focus on bank  
261 erosion, as well as on the measurements of length and width of eroded banks (mostly along the Emme River).  
262 GIS measurements were compared and validated with field observations. The width of the active channel before  
263 and after the flood and valley bottom (i.e., alluvial plain) width were calculated at several transects within each  
264 sub-reach. The centreline to the active channel polygon was obtained using the polygon to centreline tool (Dilts,  
265 2015) and perpendicular transects were obtained with the transect tool (Ferreira, 2014); width was measured  
266 based on these transects. Transects were delineated at approximately regular intervals, ranging between 20 to 50  
267 m in length, with a total of 980 transects along the stream network.

268 We calculated the confinement index ( $C_i$ ) as the ratio between the valley bottom width ( $W_{\text{valley}}$ ) to the  
269 initial channel width (pre-flood;  $W_i$ ):

$$270 \quad C_i = W_{\text{valley}} / W_i \quad [1]$$

271 and the width ratio ( $W_r$ ) as the ratio between the width of the channel post-flood ( $W_f$ ) to the channel width  
272 pre-flood ( $W_i$ ), as proposed by Krapesch et al., (2011):

$$273 \quad W_r = W_f / W_i \quad [2]$$

274 Discharge was not measured except at the outlet of the basin (Eggiwil stream gauge station; Fig.1), but  
275 estimations at other river sections were available (Table 2), using this data and the drainage area ( $A$ ) we used a  
276 potential equation to estimate peak discharges at all sub-reaches:

$$277 \quad Q = 23 \cdot A^{0.6} \quad [3]$$

278 Because the estimates using equation [3] were relatively uncertain, stream power was not calculated using  
279 the estimated peak discharge of the flood, but instead we used the stream power index proposed by Marchi and  
280 Dalla Fontana (2005) calculated as the product of the channel slope ( $S$ ) and the square root of the drainage area  
281 ( $A$ ):

$$282 \quad SPI = S \cdot A^{0.5} \quad [4]$$

283 The geomorphic response of the catchment and the initiation of processes such as LW recruitment due to  
284 mass movements or bank erosion might be driven by precipitation, among other variables (e.g., channel width,  
285 depth, and gradient). However, the rainfall patterns and subsequent disturbance regimes that influence the



286 temporal variation in LW export in a given watershed network are not yet understood fully (Seo et al., 2012,  
287 2015). Therefore, we include the event precipitation as an explanatory variable in our analysis. We hypothesize  
288 that differences in the spatial precipitation pattern would have led to differences in the geomorphic response,  
289 thereby regulating LW dynamics. The spatial and temporal distribution of the precipitation was available from  
290 the CombiPrecip database recorded by MeteoSwiss, which is calculated using a geostatistical combination of  
291 rain-gauge measurements and radar estimates with a regular grid of 1 km resolution (Sideris et al., 2014). For  
292 each sub-reach the drainage was computed as explained above, and the hourly and cumulative or total  
293 precipitation, total mean and total maximum values (i.e., the mean and maximum value of the total precipitation  
294 registered at each sub-catchment) were calculated.

295 The forest stands volumes ( $\text{m}^3\cdot\text{ha}^{-1}$ ) present before the event and eroded during the flood were assigned  
296 based on land use maps available for the study area and on information provided by the Canton of Bern and the  
297 Swiss National Forest Inventory (NFI; Brassel and Lischke, 2001) to calculate recruited wood volume (in terms  
298 of eroded vegetation; see example in Figure S4) and forested channel length. Forested channel length was  
299 determined by intersecting the forest cover with the river network. For this calculation, a wood buffer strip of 10  
300 m was added to the forest boundary to account for potential LW recruitment due to tree fall. The width of the  
301 strip was chosen to be half of the average tree height and to correspond to the area of possible location of the  
302 centre of gravity of recruited wood logs (Mazzorana et al. 2011). The dataset used for this calculation is based on  
303 the digitized topological landscape model of Switzerland 1:25,000 (source: Vector25 © 2007, swisstopo,  
304 DV033594). Recruited wood volumes were normalized by channel area (i.e.,  $\text{m}^3\cdot\text{ha}^{-1}$ ) and channel length ( $\text{m}^3\cdot\text{km}^{-1}$   
305 <sup>1)</sup> to better compare sub-reaches and compare with other studies in other regions.

306 Deposited wood was directly measured in the field as explained above and by Rickli et al. (2016). Besides  
307 the field survey and the GIS analysis, all available media data, including a video recorded from a helicopter  
308 (<http://www.heliweb.ch>), were also analysed (Zurbrügg, 2015). This analysis allowed mapping of the original  
309 depositional sites of the removed wood right after the flood and complementing the wood budget calculations.  
310 Deposited wood volumes were also normalized by channel area (i.e.,  $\text{m}^3\cdot\text{ha}^{-1}$ ) and channel length ( $\text{m}^3\cdot\text{km}^{-1}$ ) for  
311 comparisons.

312

313

314

315



316           2.3.3. *Statistical analysis*

317           First, an exploratory analysis of the potential factors at the sub-reach scale was done by applying simple  
318 linear regression and correlation (non-parametric Spearman rank test). The explanatory variables analysed were  
319 width ratio, wood recruited volume (in total volume  $\text{m}^3$ -, volume per area  $\text{m}^3\cdot\text{ha}^{-1}$ -, and volume per stream  
320 length  $\text{m}^3\cdot\text{km}^{-1}$ ) and wood deposit volume (in total volume  $\text{m}^3$ -, volume per area  $\text{m}^3\cdot\text{ha}^{-1}$ -, and volume per  
321 stream length  $\text{m}^3\cdot\text{km}^{-1}$ ). The controlling factors included were initial channel width, width ratio (for wood  
322 recruitment and deposition), channel gradient, sinuosity, confinement index, SPI, forested channel length, and  
323 total maximum and mean precipitation.

324           Sub-reaches were grouped according to their morphological characteristics, geomorphic response (using a  
325 value of width ratio  $> 1.2$  to characterize sub-reaches with important geomorphic changes in terms of channel  
326 widening), LW recruitment (sub-reaches with and without LW recruitment) and LW deposition (sub-reaches with  
327 and without LW deposition). Differences between groups of sub-reaches were tested using the non-parametric  
328 Mann Whitney (i.e., Wilcoxon signed rank test for two groups) or Kruskal Wallis (for  $> 2$  groups) tests.  
329 Significance of correlations and differences was set when p-value  $< 0.1$ .

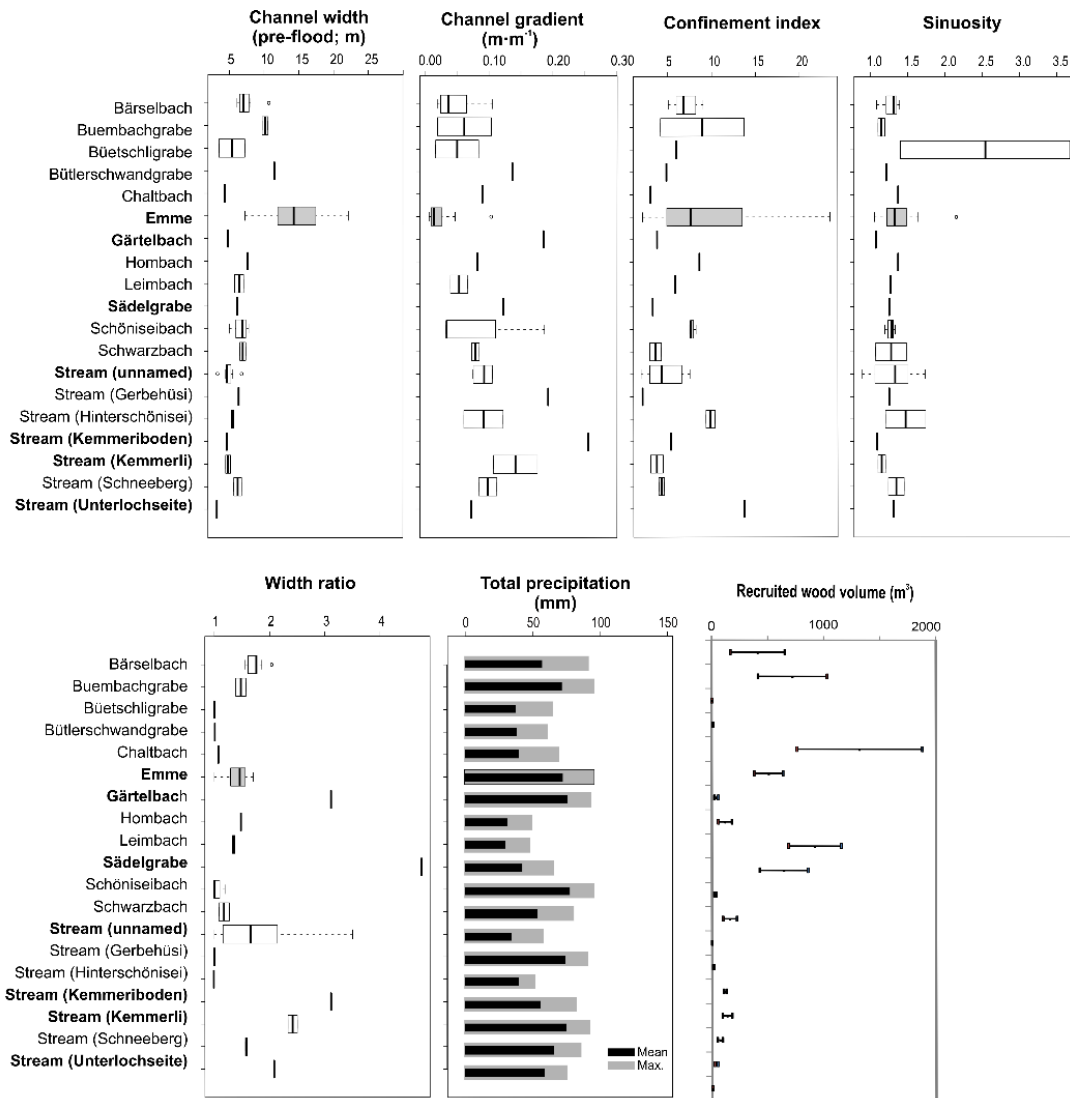
330           We hypothesize that one single variable may not explain the catchment response, but that the combination  
331 of multiple variables would. Thus, we applied multivariate analysis to estimate the probability and factors  
332 controlling channel widening, LW recruitment, and LW deposition. We applied multiple linear regression and  
333 multivariate binary logistic regression by using a stepwise approach in both cases to identify the best model based  
334 on the Akaike information criterion (AIC) and the determination coefficient. The multivariate binary logistic  
335 regression estimates the probability of a binary response (e.g., high channel widening and low channel widening,  
336 presence or absence of LW recruitment) based on different predictors (or independent) variables (e.g.,  
337 morphological variables). As the variables analysed have very different units and different orders of magnitudes,  
338 the dataset was standardized by mean-centering (the average value of each variable is calculated and then  
339 subtracted from the data, resulting in a transformed dataset in such the resulting variable has a zero mean; Becker  
340 et al., 1988) prior to computing (logistic and linear) multiple regressions. All analyses were done for all sub-  
341 reaches together, for sub-reaches along the Emme river only, and for sub-reaches along all tributaries. Variables  
342 were considered significant for p-value  $< 0.1$ .

343           Statistical analyses were carried out using the statistical software R (R Core Team, 2017) and the packages  
344 *xlsx* (Dragulescu, 2014), *Rcmdr* (Fox, 2005 and 2017; Fox and Bouchet-Valat, 2017), *corrgram* (Kevin Wright,  
345 2017), *corrplot* (Wei and Simko, 2017) and *Hmisc* (Harrell, 2016).



346 **3 Results**

347       The morphology of the sub-reaches along the Emme River and tributaries is significantly different (see  
348 Figure S5 in supplementary material), therefore we analysed their morphological response separately. Figure 3  
349 shows the averaged values for different morphological variables, the calculated width ratio and the precipitation  
350 for the 19 study streams including the Emme River reach (cf. Table 1). Looking at the different tributaries and the  
351 Emme River reach, we observe that the morphological response in terms of width ratio was very different (Figure  
352 3). The highest width ratio was observed in the Sädelgrabe, with nearly 5 times the initial channel width after the  
353 flood. The Gärtelbach and the tributary near Kemmeriboden also experienced significant channel widening.  
354 These streams were relatively narrow before the event, with initial channel widths smaller than 10 m, very steep  
355 (with channel gradients higher than 0.1), and highly confined (with confinement indices smaller than or near 5).  
356



357

358 *Figure 3: Boxplots of averaged initial channel width (before the flood), channel gradient, confinement ratio,*  
 359 *sinuosity, width ratio, precipitation and recruited wood volumes for the 19 studied streams. Total*  
 360 *maximum and mean total precipitation are calculated based on the 1 km precipitation grid cells in the*  
 361 *respective catchments (maximum shows the highest value, mean shows the mean value recorded in each*  
 362 *sub-catchment). Recruited wood volumes are given in ranges based on forest density ranges (as*  
 363 *explained in the methods). In bold streams highlighted in Figure 4.*  
 364

365

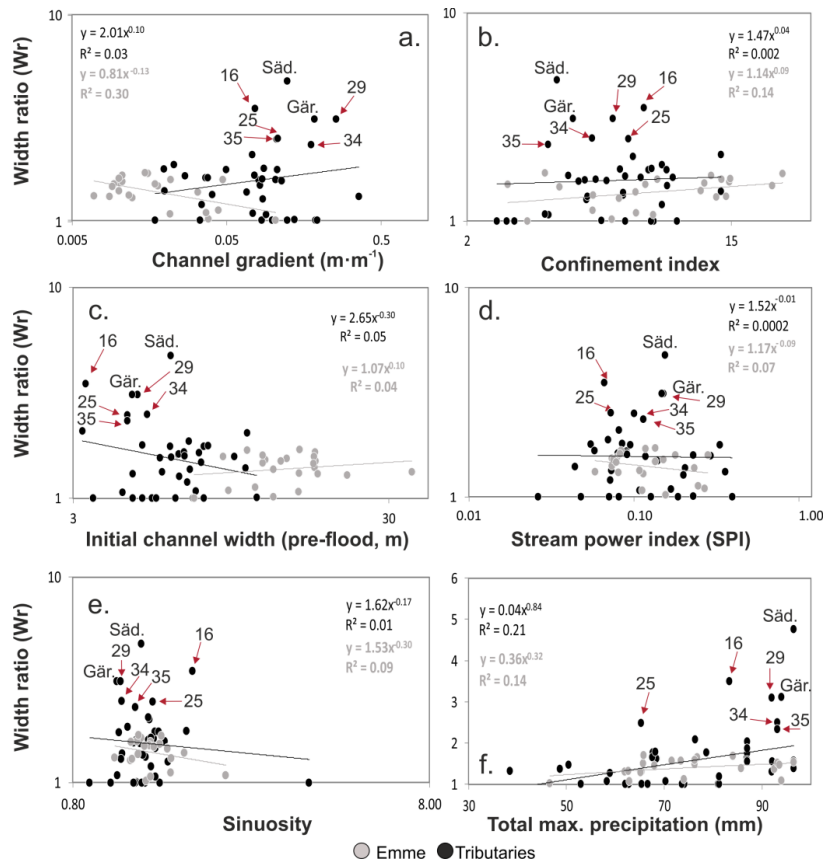
366 **3.1 Morphological flood response: channel widening**

367 The exploratory analysis of the morphological characteristics (Figure 4) showed that the relationships  
 368 between width ratio and channel gradient, confinement index, initial channel width, SPI, sinuosity and total





369 maximum precipitation variable substantially. A large scatter exists in the data, and in some cases, relationships  
 370 are very different for the Emme sub-reaches and for the tributaries sub-reaches.

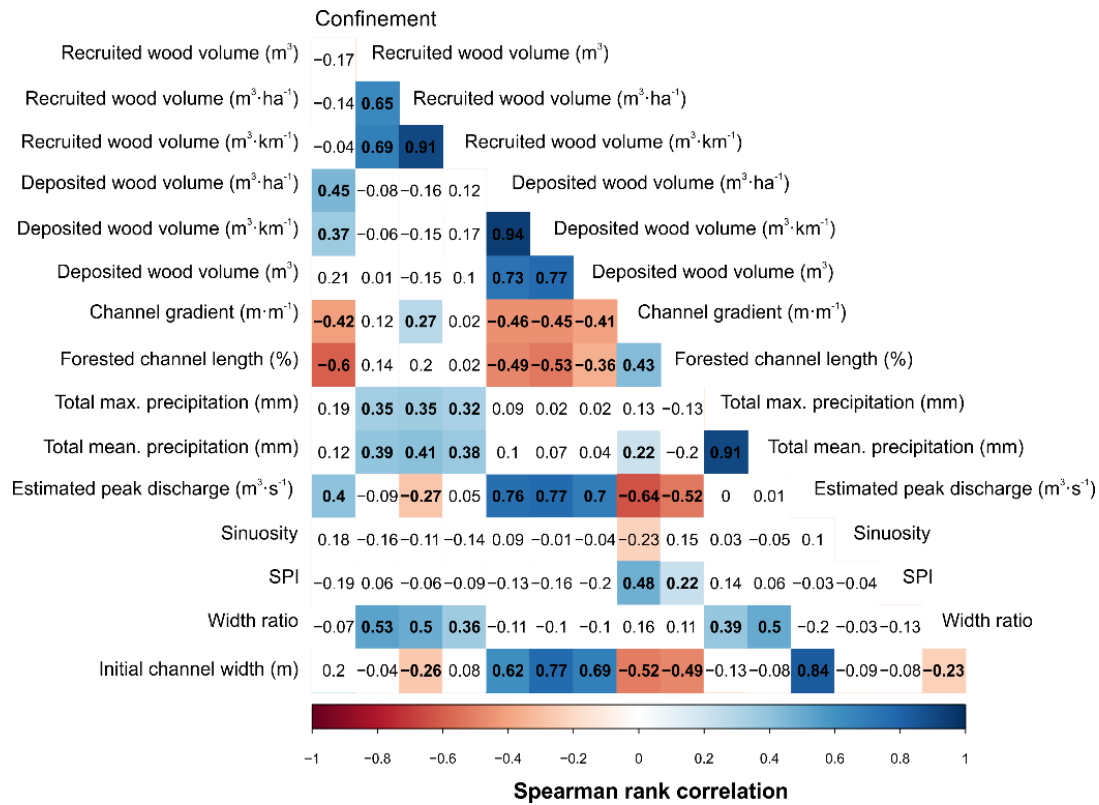


371

372 *Figure 4: Relationships between width ratio and (a) channel gradient; (b) confinement; (c) channel width (pre-*  
 373 *flood); (d) stream power index (in  $m^{-1} \cdot km^2$ ); (e) sinuosity; (f) total maximum precipitation. Grey dots*  
 374 *show sub-reaches along the Emme River, black dots show sub-reaches along tributaries. Säd.:*  
 375 *Sädelgrabe; Gär.: Gärtelbach; numbers are sub-reaches as shown in Table 1. Grey and black lines show*  
 376 *regression lines for the Emme River sub-reaches and tributaries sub-reaches respectively. Note that*  
 377 *panel f has a linear x-axis in contrast to the logarithmic x-axis of panels a-e.*  
 378

379 According to the Spearman rank test for all sub-reaches together (Figure 5) and for the tributaries sub-  
 380 reaches (Figure S7), a significant positive correlation was found between width ratio and the total maximum and  
 381 mean precipitation. Forested channel length was also significantly correlated to channel widening along the  
 382 Emme sub-reaches (Figure S8).

383



384

385 *Figure 5: Spearman rank correlation matrix of all variables included in the analyses and for all sub-reaches*  
 386 *together. Values shows the Spearman rank results (significant correlations are in bold). Red colours*  
 387 *show significant negative correlations, blue shows significant positive correlation, white shows*  
 388 *insignificant correlations.*  
 389

390 When sub-reaches without widening (i.e., width ratio < 1.2) are removed from the correlation analysis,  
 391 other significant correlations besides precipitation were observed (Table 3), such as channel gradient and initial  
 392 channel width. Hence, the inclusion of sub-reaches which did not experience widening changed results, a fact that  
 393 is discussed further in section 4.

394



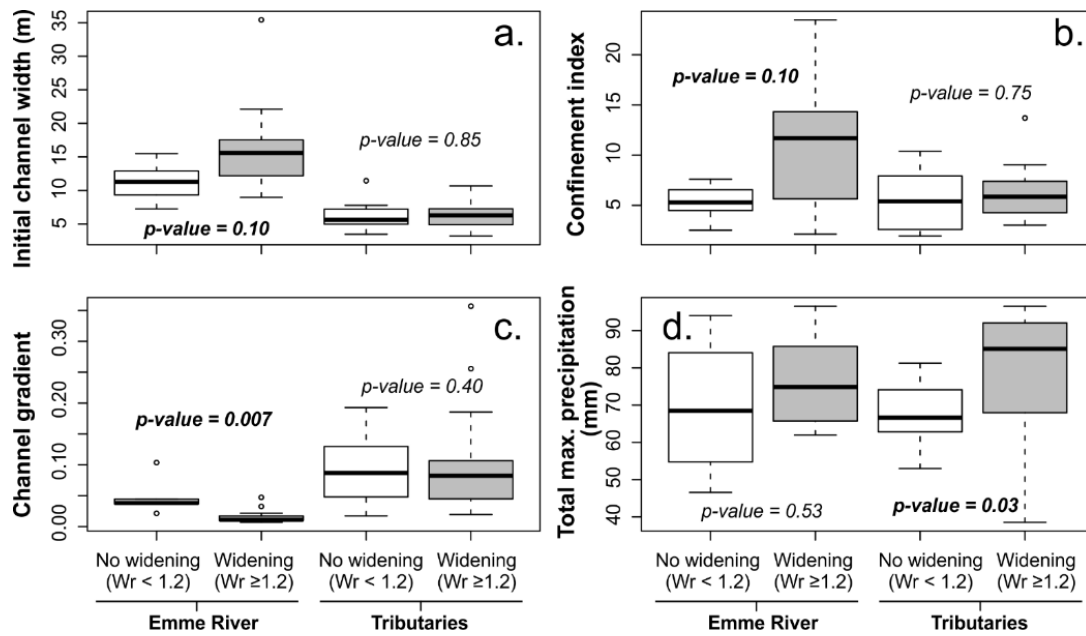
395 *Table 3: Spearman Rank correlation matrix for the width ratio versus different variables and for all sub-reaches,*  
 396 *only Emme sub-reaches and only tributaries sub-reaches only with sub-reaches showing widening (i.e.,*  
 397 *width ratio > 1.2). Bold indicates significant correlation.*  
 398

Width ratio	Variables (All sub-reaches with width ratio > 1.2)	Variables (Emme sub-reaches with width ratio > 1.2)	Variables (Tributaries sub-reaches with width ratio > 1.2)
Confinement index	-0.12	0.22	-0.06
<b>Channel gradient</b>	<b>0.46</b>	0.33	0.26
<b>Total max. precipitation (mm)</b>	<b>0.35</b>	<b>0.40</b>	0.31
<b>Total mean precipitation (mm)</b>	<b>0.32</b>	<b>0.48</b>	<b>0.38</b>
Sinuosity	-0.06	0.08	-0.09
Forested channel length (%)	0.22	-0.18	-0.06
<b>Initial channel width (m)</b>	<b>-0.56</b>	<b>-0.49</b>	<b>-0.43</b>
SPI	-0.08	0.27	-0.23

399

400 We compared the sub-reaches showing widening (i.e., width ratio > 1.2) with the sub-reaches not showing  
 401 widening (i.e., width ratio < 1.2) and results revealed significant differences between these two groups (see also  
 402 Figure S6) and between sub-reaches along the Emme and along tributaries (Figure 6). We find that sub-reaches  
 403 with a large width ratio were significantly less confined (high values of confinement index), less steep and  
 404 received a much higher precipitation during the storm. By contrast, sub-reaches where widening was important  
 405 were also wider (channel width before the flood) and less forested, however, these differences were not  
 406 significant. Interestingly, analysis of the sub-reaches along the Emme and along the tributaries independently  
 407 showed similar trends (Figure 6).

408



409

410 *Figure 6: Boxplots of morphological variables (initial channel width, confinement index, channel gradient) and*  
 411 *total maximum precipitation for all sub-reaches showing widening (i.e., width ratio  $\geq 1.2$ ; grey boxes)*  
 412 *and sub-reaches not showing widening (i.e., width ratio  $< 1.2$ ). The bottom and top of the box indicate*  
 413 *the first and third quartiles, respectively, the black line inside the box is the median and circles are*  
 414 *outliers. The Wilcoxon signed rank test result (*p*-value) for the significance of differences is also shown,*  
 415 *bold indicates significant differences.*  
 416

417 The logistic regression points to an increase in the probability of widening occurrence with increasing  
 418 precipitation and confinement index. On the other hand, the probability of channel widening decreases with an  
 419 increase in channel gradient, sinuosity, SPI, and forested channel length for all sub-reaches together. As with  
 420 previous results, the sub-reaches along the Emme and along tributaries showed a contrasting behaviour. Along  
 421 the Emme, widening probability increased for wider, gentler, less sinuous, and less forested sub-reaches, whereas  
 422 in the case of tributaries, the probability for the channels to widen was larger for narrower, steeper, sinuous  
 423 forested sub-reaches.

424 The role of precipitation is univocal in all cases, confirming our initial hypothesis about the role of the  
 425 spatial distribution of precipitation. The logistic stepwise procedure revealed that the most significant variables  
 426 explaining widening probability for all sub-reaches were total maximum precipitation, SPI, and estimated peak  
 427 discharge (Table S1). Results obtained for sub-reaches along the Emme showed that forested channel length was  
 428 also significant to explain widening.

429 The multiple linear regression between width ratio values and the same explanatory variables for all sub-  
 430 reaches identified precipitation, gradient and SPI as significant variables. However, obtained models explained



431 only between 14 and 19 % of the variability (Table S2). Separate multiple linear regression models for sub-  
 432 reaches along the Emme and along tributaries further identify forested channel length, sinuosity, and initial  
 433 channel width as significant variables; overall, models explained between 20 and 50% of widening variability.

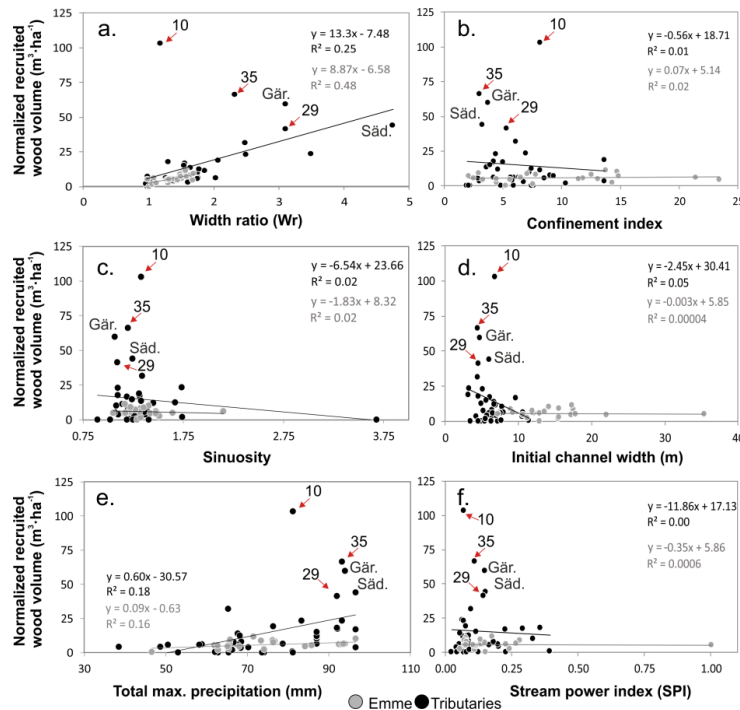
434

435

### 436 3.2 Large wood recruitment and deposition

#### 437 3.2.1. Factors controlling large wood recruitment

438 The most important sources of LW were the tributaries Bärselbach, Buembachgrabe, Gärtelbach, and  
 439 Sädelgrabe, together with the main river Emme (see Figure 3). To understand the factors controlling LW  
 440 recruitment at the sub-reach scale better, we explored correlations between different variables and the total LW  
 441 volume, as well as the normalized recruited wood volume per stream hectare (Figure 7) and per channel length.  
 442 In these analyses, we also included sub-reaches without LW recruitment.



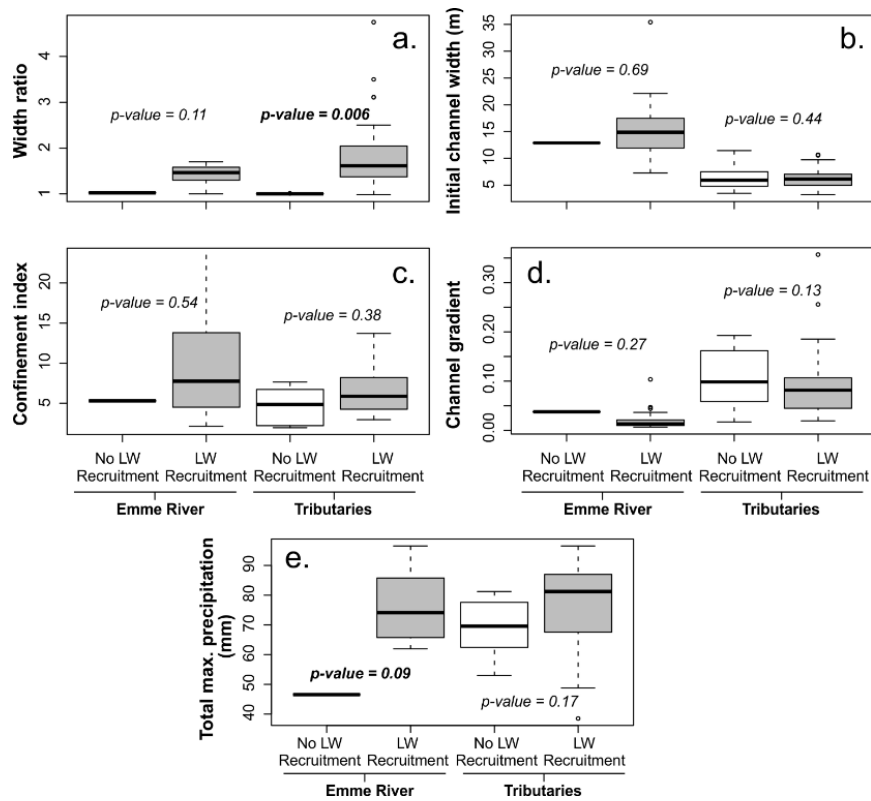
443

444 *Figure 7: Relationships between recruited wood volume normalized by stream hectare ( $\text{m}^3 \cdot \text{ha}^{-1}$ ; mean value*  
 445 *according to mean value of forest density) and (a) width ratio; (b) confinement index; (c) sinuosity; (d)*  
 446 *initial channel width (m); (e) total maximum precipitation (mm) and (f) SPI. Grey and black lines show*  
 447 *regression lines for the Emme river and tributaries sub-reaches respectively. Sädelgrabe; Gär. =*  
 448 *Gärtelbach; numbers correspond to sub-reaches as shown in Table 1.*  
 449



450 Even though the results showed a large scatter, some relationships can be identified. For instance, we  
451 found a positive significant correlation between recruited wood volume ( $\text{m}^3$ ,  $\text{m}^3 \cdot \text{ha}^{-1}$  and  $\text{m}^3 \cdot \text{km}^{-1}$ ) and width ratio  
452 (Figure 5). This confirms that bank erosion (i.e., channel widening) was the main recruitment process. Again,  
453 sub-reaches receiving larger amounts of precipitation recruited higher quantities of LW and we observe a  
454 statistically significant positive correlation between total maximum and mean precipitation and recruited wood  
455 volume (for all three recruited wood volume variables). This is explained by the control of precipitation driving  
456 discharge, and thus driving the widening of channels and the wood recruitment process. Channel morphology  
457 may play a role in wood recruitment as well; we observe a significant negative correlation between recruited LW  
458 volume and initial channel width and a significant positive correlation with channel gradient (Figure 5).  
459 However, these significant correlations were found only for wood volume per stream hectare and not for total  
460 wood volume or wood volume per stream length (Figure 5).

461 Independent analyses for sub-reaches along the Emme or along tributaries showed similar results  
462 (correlation matrices shown in Figures S7 and S8). We also performed the same analysis with sub-reaches  
463 showing LW recruitment (i.e., removing those in which no LW was recruited) and found similar results in terms  
464 of significant correlations with the different variables (results not shown here). However, the comparative  
465 analysis of sub-reaches with and without LW recruitment (Figure 8) revealed that LW recruitment was observed  
466 primarily in sub-reaches characterized by a significantly greater confinement index (i.e., unconfined sub-reaches)  
467 and significantly smaller slope.



468

469 *Figure 8: Boxplots of morphological characteristics (width ratio, initial channel width, confinement index,*  
 470 *channel gradient and), total max. precipitation of sub-reaches showing wood recruitment and not*  
 471 *showing LW recruitment. The bottom and top of the box indicate the first and third quartiles,*  
 472 *respectively, the black line inside the box is the median and circles are outliers. The Wilcoxon signed*  
 473 *rank test result (p-value) for the significance of differences is also shown, bold indicates significant*  
 474 *differences.*  
 475

476 Figure 8 shows that sub-reaches with LW recruitment were in general wider and with sub-reaches longer  
 477 forested lengths than sub-reaches with no LW recruitment, however, differences were not significant (the results  
 478 of all sub-reaches together, without grouping sub-reaches along the Emme and along tributaries are shown in  
 479 Figure S9).

480 The logistic regression allowed calculation of the probability of LW recruitment occurrence. According to  
 481 results, the probability of LW recruitment increases with channel widening and precipitation; and decreases with  
 482 initial channel width and channel gradient. However, none of the variables were significant (Table S3), and the  
 483 final stepwise logistic regression model selected just width ratio and confinement index as variables explaining  
 484 LW recruitment probability.

485 The multiple linear regression points to total maximum precipitation and width ratio as the most significant  
 486 variables explaining total LW recruitment volume (total m<sup>3</sup>) variability, but forested channel length was also



487 included in the final stepwise regression model for all sub-reaches. Between 10 and 32 % of the variability was  
 488 explained by these models (adjusted  $R^2$ ) (Table S4).

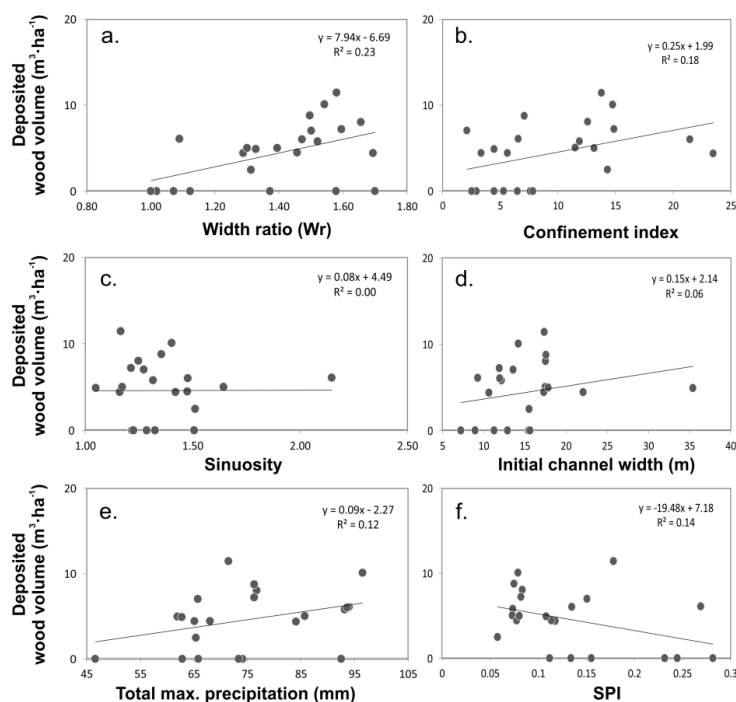
489

490

### 491 3.2.2. Large wood deposition along the Emme River

492 LW deposits were analysed along the Emme River and its tributary Sädelgrabe. However, because LW was  
 493 mostly deposited on the Sädelgrabe fan and piled up nearby, only results obtained along the Emme sub-reaches  
 494 can be provided here. The exploratory analysis of LW deposit distribution showed a positive relationship between  
 495 deposited wood volume (normalized by stream area;  $\text{m}^3 \cdot \text{ha}^{-1}$ ) and width ratio, confinement index, initial channel  
 496 width, and total precipitation; and a negative relationship with SPI (Figure 9).

497



498

499 *Figure 9: Relationships between deposited wood volume per stream hectare ( $\text{m}^3 \cdot \text{ha}^{-1}$ ) along the Emme River sub-*  
 500 *reaches and (a) width ratio; (b) confinement index; (c) sinuosity; (d) channel width pre-flood; (e) total*  
 501 *maximum precipitation (mm); and (f) SPI.*

502

503 The Spearman test yielded a negative significant correlation of deposited LW with channel gradient and  
 504 SPI, and a positive correlation with estimated peak discharge (Figure 5). By contrast, the confinement index and

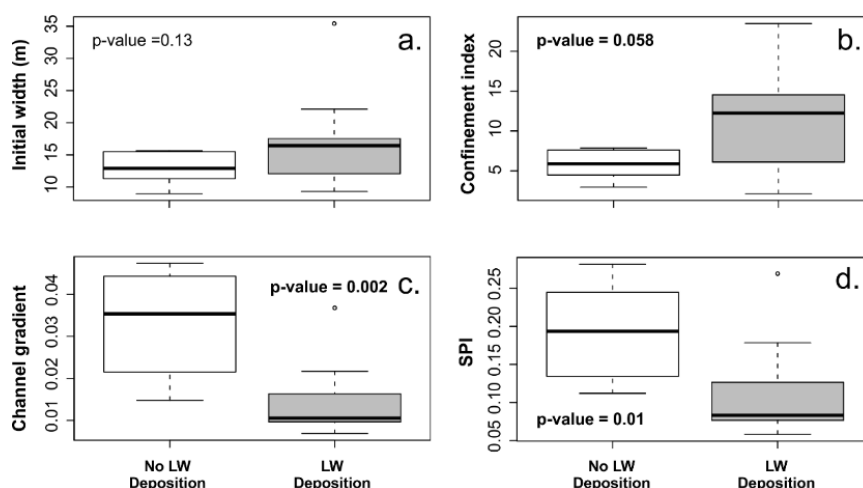




505 initial channel width were only significantly correlated with deposited LW volume per hectare and per kilometre,  
506 respectively.

507 The comparison between Emme sub-reaches where LW was deposited or not showed statistically  
508 significant differences in terms of confinement index, channel gradient, and SPI (Figure 10).

509



510

511 *Figure 10: Boxplots of morphological characteristics (initial channel width, confinement index, channel*  
512 *gradient, and SPI), of sub-reaches showing and not showing LW deposition along the Emme river. The*  
513 *bottom and top of the box indicate the first and third quartiles, respectively, the black line inside the*  
514 *box is the median and circles are outliers. The Wilcoxon signed rank test result (p-value) for the significance*  
515 *of differences is also shown, bold indicates significant differences.*  
516

517 The probability of LW deposition estimated by logistic regression confirmed that LW deposition  
518 probability increases with increasing width ratio, confinement index, and initial channel width, whereas it  
519 decreases with increasing channel gradient and SPI. The multivariate stepwise logistic regression model  
520 identified both the confinement index and estimated peak discharge as significant variables explaining LW  
521 deposition, but also included the width ratio in the final model (Table S5).

522 The multiple linear regression of LW deposited volume (i.e. total  $m^3$  and  $m^3$ ,  $m^3 \cdot ha^{-1}$  and  $m^3 \cdot km^{-1}$ ) showed  
523 that the significant variables include channel gradient, estimated peak discharge, initial channel width, SPI, and  
524 confinement index (Table S6). The models explained between 51% and 67% of the variance. The largest  
525 variability (70%) was explained for LW deposited volume per stream length ( $m^3 \cdot km^{-1}$ ).

526

527

528



529 **3.3. Large wood budget and size distribution**

530 LW budget was fully analysed along the lower part of the surveyed Emme River and the Sädelgrabe  
 531 tributary. This tributary delivered large quantities of LW by mass movements and debris flows, which was mostly  
 532 deposited along its fan and the Emme River, however, and according to eyewitness reports, a substantial amount  
 533 of LW was also transported further downstream and to clog the Räbloch gorge. At this narrow canyon (Fig. 1),  
 534 wood and additional debris created a dam of 8 to 10 m in height.

535

536 *Table 4: Wood budget along the Sädelgrabe. Uncertainties of up to 50% are included in the stated volumes.*

537  
 538

Processes	Recruited (m <sup>3</sup> )	Deposited (m <sup>3</sup> )	Exported (m <sup>3</sup> )
Landslides/bank erosion	331 ± 66		
Previously deposited in channel	150 ± 75		
Stored in the piles close to the confluence		100 ± 20	
Extracted before survey		32 ± 11	
Deposited on the fan (forests)		172 ± 34	
Deposited on the fan (pastures)		25 ± 9	
Subsequently deposited in channel (after event)		100 ± 50	
Stored in pile at fan apex		30 ± 15	
Exported to the Emme			40 ± 20
<b>Total</b>	<b>481 ± 141</b>	<b>458 ± 139</b>	<b>40 ± 20</b>

539

540 Recruited LW volumes in the Sädelgrabe were due to landslides and bank erosion; the LW volume was  
 541 estimated to be equal to 331 m<sup>3</sup> (Table 4), together with the estimated volume of wood stored within the channel  
 542 before the event (150 m<sup>3</sup>), we obtained in 481 m<sup>3</sup> of recruited and entrained wood. About 458 m<sup>3</sup> of wood was  
 543 deposited at various locations (172 m<sup>3</sup> were deposited on the fan, 100 m<sup>3</sup> were piled up along the stream bed and  
 544 the municipal road and 100 m<sup>3</sup> were remaining in the stream bed of the Sädelgrabe after the event). Our  
 545 estimations showed that only a small volume (about 40 m<sup>3</sup>) was exported from the Sädelgrabe to the Emme  
 546 River.

547 Another source of LW was the Gärtelbach, which delivered large quantities of LW directly to the Emme  
 548 River, of which most was deposited along the floodplain in the vicinity of the Schwand bridge. The total volume  
 549 of wood estimated in this area was 250 m<sup>3</sup>. Table 5 summarizes the wood budget computed along one segment of  
 550 the Emme river.

551



552

553 *Table 5: Wood budget along the lower reach of the studied Emme River segment. Uncertainties of up to 50% are*  
 554 *included in the stated volumes*  
 555

Processes	Recruited (m <sup>3</sup> )	Deposited (m <sup>3</sup> )	Exported (m <sup>3</sup> )
Bank erosion along the studied reach	192±38		
Previously deposited	100 ± 50		
Piles close to Bumbach			
Deposited along the river		360	
Temporary storage in Bumbach			360 ± 36
Stored jam in Räßloch gorge		480 ± 45	
Input from Sädelgrabe	40 ± 20		
<b>Total</b>	<b>332</b>	<b>833 ± 64</b>	<b>360 ± 36</b>

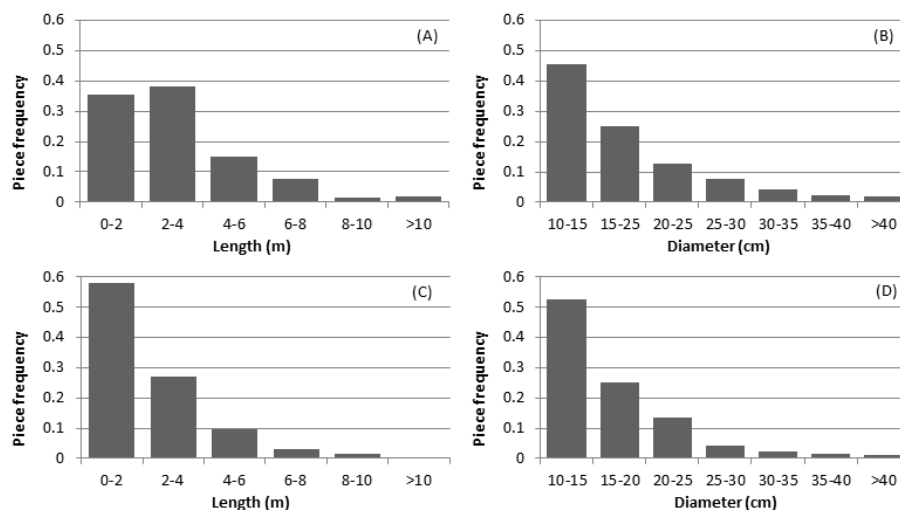
556

557 Bank erosion along the surveyed Emme River segment recruited about 192 m<sup>3</sup> of wood, that together with  
 558 the estimated previously stored wood (100 m<sup>3</sup>) and the input from the Sädelgrabe was summed at 332 m<sup>3</sup>.  
 559 Roughly 250 m<sup>3</sup> were deposited in an area near Schwand, and the rest along the Emme River. The sum of the  
 560 deposited wood was approximately 360 m<sup>3</sup>. In addition, about 300 m<sup>3</sup> of LW from flooded areas were transported  
 561 to a landfill as part of clean-up work and post event measures. Another important element of the balance is a  
 562 large jam of approximately 480 m<sup>3</sup> of wood, which formed about 1.6 km downstream of the investigated section  
 563 at Räßloch. Unfortunately, it is not known how much wood was transported from the upper reaches above  
 564 Kemmeriboden into the considered section, and therefore a mismatch exists between the estimated recruited,  
 565 deposited, and exported volumes.

566 Pieces of LW were surveyed and measured both along the Emme sub-reaches between Kemmeriboden and  
 567 Räßloch (Figure 1) and along the Sädelgrabe tributary. In total, 1995 (i.e. 1658 along the Emme and 297 on the  
 568 Sädelgrabe fan and nearby piles) pieces were measured and the size distribution was further analysed (Figure 11).  
 569 For both the Sädelgrabe and Emme River, piece frequency generally decreases with increasing piece length and  
 570 diameter. Regarding the relative diameter distribution, almost no differences exist between the two sites, and in  
 571 both cases the range class of 10-15 cm is the most frequent with approximately 50% of the total. The mean and  
 572 median values of piece length and diameter are very similar in the Emme River (mean D: 16.6 cm, mean L: 4.04  
 573 m / median D: 15 cm, median L: 2.32 m) and Sädelgrabe torrent (mean D: 17.4 cm, mean L: 3.06 m; median D:  
 574 15 cm, median L: 2.5 m). Regarding the relative length distribution, short wood pieces (<2 m) were more  
 575 frequently found along the Emme River (almost 60 %), whereas longer pieces (>2 m) were more prevalent along



576 the Sädelgrabe (around 60 %). However, the longest piece was found in the Emme (20.7 m), while the longest  
577 piece measured in the Sädelgrabe was substantially shorter with a value of 12.0 m.  
578



579

580 *Figure 11: Size distribution (piece diameter and length) of deposited LW pieces in the Sädelgrabe (a) and (b) and*  
581 *in the Emme River (c) and (d). In all panels the bars relate to the relative frequency of pieces.*  
582

583

## 584 4 Discussion

### 585 4.1. Channel response to the 2014 flood

586 In this study, we presented an integration of different approaches and data sources (i.e., field survey, GIS-  
587 remotely sensed data and statistical analysis) at different spatial scales to better understand flood response in  
588 terms of channel widening and LW dynamics. We proved the importance of performing an overall analysis over  
589 the entire catchment, although the flood event and responses to it were restricted to some areas of the catchment  
590 only. This approach allowed identification of hydrometeorological and geomorphic thresholds for channel  
591 widening, LW recruitment, and deposition. The inclusion of sub-reaches without important widening or without  
592 LW recruitment and deposition in the analysis showed that sub-reaches with similar characteristics may exhibit  
593 significantly different responses during the same event, and that variables explaining these responses may not be  
594 identified properly if only one part of the dataset is analysed.



595 Previous works observed that hydraulic forces (e.g., stream power) are not sufficient to explain  
596 geomorphic effects of floods (Nardi and Rinaldi, 2015), and other variables, such as initial channel width,  
597 confinement or human interventions should be included in assessments (Surian et al., 2016 and references  
598 therein). We confirmed with this study that the flood triggering precipitation is key in understanding the  
599 magnitude and spatial variability of catchment response and that it should thus be included in future analyses. As  
600 hypothesized, differences in spatial precipitation patterns led to differences in the geomorphic response of the  
601 catchment, regulating channel widening and thereby controlling LW dynamics. Albeit this observation may have  
602 been expected, it has rarely been addressed in post-event surveys (Rinaldi et al., 2016) even in cases where data  
603 was available at the proper spatial scale (e.g., Surian et al., 2016).

604 Precipitation was the univocal variable to explain channel widening in statistically significant terms,  
605 provided that all sub-reaches were including, or whenever only sub-reaches along the Emme River or along  
606 tributaries were analysed. A threshold value of around 80 mm precipitation was observed in sub-reaches with the  
607 most important widening (Fig. 4). When sub-reaches without widening were removed from analysis, channel  
608 morphology (in terms of initial channel width, confinement and gradient) and hydraulic conditions (i.e., estimated  
609 peak discharge) were also significantly correlated with the width ratio. In fact, sub-reaches with a confinement  
610 index larger than 10 (i.e., unconfined channels) and wider than 10 m experienced less widening. This means that  
611 after intense precipitation events, channel morphology is a secondary driver for channel widening. Initial channel  
612 width was significantly negatively correlated with width ratio, as previously observed by Surian et al. (2016),  
613 Comiti et al. (2016) and Righini et al. (2017), who analysed reaches that showed important widening in several  
614 streams in Italy. These authors also found the confinement index to be an important variable controlling channel  
615 widening. Regarding this variable, we observed contrasting a behaviour in the sub-reaches along the Emme River  
616 (where the width ratio was positively correlated with the confinement index) and along tributaries (where the  
617 width ratio was negatively correlated with the confinement index). This is because the largest widening was  
618 observed along tributary sub-reaches, which are relatively more confined than the main river. In fact, only along  
619 the Emme River we observed that sub-reaches showing channel widening were significantly less confined than  
620 sub-reaches not showing widening at all. In contrast, differences were not significant along the tributaries. This  
621 apparently contradictory result might be explained by several reasons. First, some large width ratios derived from  
622 aerial pictures (i.e., only on planimetric observations) may possibly include erosion of parts of the adjacent  
623 hillslopes, a process that also occurs during the flood. This was observed along the Sädelgrabe, where some  
624 highly confined transects showed widening ratios exceeding the confinement index (as also observed by Comiti



625 et al., 2016). One may argue that these slope failures should not be considered as channel widening, because the  
626 process here is more related to hillslopes movements (e.g., falls, slips, slabs, slumps) than to channel processes.  
627 Second, some of the tributaries, especially the Sädelgrabe and Gärtelbach, received the highest amounts of  
628 precipitation, resulting in a more intensive response. However, logistic regression showed that widening  
629 probability increased with increasing confinement index. Besides channel confinement, lateral constraints, mainly  
630 artificial rip-raps or channelization, or natural bedrock, were present before the flood occurred, especially along  
631 the Emme River (see Figure S2). These natural or artificial lateral constraints were not explicitly included in the  
632 analysis; however, they may have influenced results (Hajdukiewicz et al., 2015; Surian et al., 2016), therefore  
633 blurring factors controlling these processes and making their identification more difficult. In addition, major  
634 adjustments occurred during the last century, mostly channel narrowing and channel planform changes. These  
635 changes occurred at tributary confluences and along some of the Emme River sub-reaches, especially in  
636 unconfined sub-reaches where the stream changed from a braided to a single-thread pattern (Figure S2). These  
637 anthropogenic changes may have an influence on current river response to floods and should thus be taken into  
638 account as well. Historical analyses were out of the scope of this study, however, they provided key information  
639 to assess whether and to what extent the response of a flood may involve channel segments that experienced  
640 significant changes in historical times (Rinaldi et al., 2016).

641 As shown in the results, sub-reaches along tributaries experiencing large channel widening were  
642 significantly steeper than those without widening, while along the Emme River channel, widening happened  
643 mostly along the gentler sub-reaches. This contrasting effect is explained by the same reasons exposed above  
644 regarding widening and confinement. A negative correlation between width ratio and channel gradient as found  
645 along the flatter Emme River reaches was also observed by Lucía et al. (2015), however, channel gradient is  
646 much smaller along the Emme River than in the Italian streams analysed by these researchers. The hydraulic  
647 conditions represented here by the estimated discharge and the SPI were not found to be significantly correlated  
648 with width ratio, although the multiple linear regression identified SPI as a significant variable explaining  
649 channel widening. Due to the large uncertainties related to the estimation of peak discharge at each transect and  
650 sub-reach, we preferred not using total stream power or unit stream power for analysis, but selected SPI instead.  
651 However, even when accurate discharge estimates are available, stream power has been shown to only partially  
652 explain channel changes, as other factors might be more relevant (Krapesch et al., 2011, Comiti et al., 2016,  
653 Surian et al., 2016; Righini et al., 2017). Finally, another morphological variable included in our analysis was  
654 sinuosity. However, this variable was not significant and did not explain channel widening, even though the



655 logistic regression revealed that widening probability may increase for medium sinuous sub-reaches. Nardi and  
656 Rinaldi (2015) also found higher width ratios for braided and wandering reaches than for straight or highly  
657 sinuous reaches.

658 Besides channel morphology, the presence of vegetation also influenced channel response. Forested  
659 channel length was negatively correlated with width ratio, sub-reaches that experienced large widening were  
660 significantly less forested than those not experiencing channel widening. This illustrates the role of vegetation in  
661 protecting riverbanks from erosion (Abernethy and Rutherford, 1998). Other variables such as bank material  
662 (e.g., cohesive, non-cohesive, bedrock), type of vegetation, and vegetation density were not included in our  
663 analysis although they can be important factors affecting flood response; they should therefore be considered in  
664 future analyses.

665

666

#### 667 4.2. LW recruitment and deposition during the flood

668 LW recruitment was controlled primarily by bank erosion (i.e., channel widening) and thus, factors  
669 controlling this process were identified as significant factors for LW recruitment. We observed a significant  
670 correlation between LW recruited volume and width ratio, precipitation, initial width, and channel gradient (i.e.  
671 the correlation with the last two variables was significant just for volume of wood recruited per channel hectare).  
672 The confinement index was also included in the final logistic regression model. There are not many previous  
673 studies that analysed LW recruitment after a single large flood. At the time of writing this manuscript, only the  
674 work of Lucía et al. (2015) was available, reporting on results from Northern Italy. The 2011 flood in the Magra  
675 river basin recruited large amounts of LW as well, mostly by bank erosion too. In their work, the authors did not  
676 find many significant correlations for total recruited wood volume, only a negative correlation with channel  
677 gradient. Our findings agree with their study and confirm the important role of bank erosion in recruiting wood  
678 material in mountain rivers, thereby highlighting that hillslope processes were not the dominant LW supplier  
679 (contrary to what was proposed by Rigon et al., 2012).

680 This means that more attention should be paid to the understanding of bank erosion processes and the  
681 interactions with vegetation to predict or identify LW recruitment sources. Our findings also revealed that  
682 morphological variables alone may not explain or predict LW recruitment, and that other factors should be  
683 considered as well, such as the triggering precipitation of the recruitment processes. As expected, the percentage



684 of forested channel was also significant in the multiple linear regression model. However, other vegetation  
685 characteristics could play a role, such as the type and density of vegetation (Ruiz-Villanueva et al., 2014).

686 In our study, LW deposition was controlled mostly by channel morphology. We found significant  
687 correlations between LW deposited volume and initial channel width, channel gradient and SPI. Sub-reaches  
688 where LW was deposited were significantly less confined (mainly in sub-reaches with confinement index higher  
689 than 7), wider (LW deposit was enhanced in sub-reaches wider than 15 m), and gentler than sub-reaches with no  
690 LW deposits. According the multiple linear regression model, 67 % of the variance was explained by these  
691 variables. These results are contrasting with those found by Lucía et al. (2015), who did not find any statistically  
692 significant relationship with the controlling variables, although they observed that LW was more pronounced in  
693 the wider, milder slope reaches, typically located in the lower river sections (Lucía et al., 2015). However, in  
694 their case, LW deposition was severely affected by the presence of several bridges and the formation of new in-  
695 channel islands due to bed aggradation.

696 We could compute wood budgets just for one tributary (Sädelgrabe) and one segment of the Emme river.  
697 Similarly to what is commonly done for sediment transport, a wood budget for a river basin should be a  
698 quantitative statement of the rates of recruited (delivered), deposited, and transported wood volumes (Benda and  
699 Sias, 2003). Detailed quantitative information about previously stored wood in the river channels was not  
700 available and we therefore had to assume that a value of 100 m<sup>3</sup> was reliable for this area based on previous  
701 studies (Rickli und Bucher 2006). In addition, the budget for the Emme river segment was not completed, as we  
702 could not compute all elements (e.g., previously stored wood, deposited wood during the flood) of the budget in  
703 all sub-catchments upstream. Computing wood budgets at the catchment scales is very challenging but might be  
704 crucial for the proper management of river basins and when it comes to wood-flood hazard mitigation (Comiti et  
705 al., 2016).

706 Regarding the size of deposited logs, the median diameter observed in the field was equal to 15 cm and the  
707 median length was equal to 2.3 m and 2.5 m in the Sädelgrabe and Emme River, respectively. These values were  
708 slightly smaller than values observed after the flood in August 2005 in central Switzerland (Steeb et al., 2017;  
709 Rickli et al., 2018), or after the flood in the Magra river (although only log length was reported by Lucía et al.,  
710 2015), but in line with logs deposited along several streams in the Italian Alps (Rigon et al., 2012). We found  
711 smaller pieces along the Emme River as compared to the Sädelgrabe, indicating that pieces in the Emme may  
712 have travelled longer distances, and that pieces have been broken during transport.





713 The flood event analysed here was a large flood, and although the recruited and transported LW resulted in  
714 significant damage (i.e., clogging bridges and damaging buildings), the exported volume was not extremely high.  
715 According to our estimations, most LW recruited in the Sädelgrabe (480 m<sup>3</sup>) and along the lower reach in the  
716 Emme River (890m<sup>3</sup>) was not transported long distances downstream but deposited nearby its source. Part of the  
717 material was clogged in the Räbloch gorge (between the villages of Schangnau and Eggwil) including the woody  
718 material from the bridge destroyed at Bumbach. Still, LW was transported further downstream and stored in  
719 several hydropower dams and reservoirs along the Aare (downstream its confluence with the Emme river).  
720 According to the dam managers' estimations, a total of 1500 m<sup>3</sup> of wood was stored in five dams. However, it  
721 was not possible to compute precise budgets for the entire Emme catchment and its tributaries, and this value thus  
722 needs to be confirmed. Nevertheless, the exported LW volume in our study can be classified as very low when  
723 compared with volumes transported during the flood in August 2005 in Switzerland (Steeb et al., 2017) and with  
724 other events, as illustrated in the review by Ruiz-Villanueva et al. (2016).

725 Due to the complexity inherent to channel widening and LW dynamics, predictions on the location of  
726 major geomorphic changes and the magnitude of LW recruitment during large floods are very challenging  
727 (Buraas et al., 2014; Surian et al., 2016). Documenting events like the one reported here is fundamental for a  
728 better understanding of the processes involved and for the development of reliable and robust tools and  
729 approaches to facilitate the inclusion of such processes in flood hazard assessments (Comiti et al., 2016). As  
730 such, a real need exists to complement current inundation mapping with a geomorphic approach (Rinaldi et al.,  
731 2015 and 2016; Righini et al., 2017) and an integrative analysis of LW dynamics (Mazzorana et al., 2017).

732

733

## 734 5. Conclusions

735 Channel widening and LW dynamics are usually neglected in flood hazard mapping and river basin  
736 management. However, the present study clearly shows the importance of these processes during floods in  
737 mountain rivers. Still, a proper identification of factors controlling river basin response remains challenging. In  
738 that regard, our results also show that the identification of significant variables may be difficult, and that  
739 depending on how the data is collected and analysed (e.g., whether non-affected sub-reaches are included or not  
740 or which variables are considered), different outcomes are possible. However, we also showed that precipitation  
741 and variables such as forested channel length may play an important role in explaining flood response, and that  
742 they should thus be taken into consideration. Precipitation was the univocal statistically significant variable to



743 explain channel widening, and only when sub-reaches without widening were removed from the analysis, channel  
744 morphology (i.e. initial channel width, confinement, and gradient) and hydraulic conditions (in terms of estimated  
745 peak discharge) were also significantly correlated with width ratio. LW recruitment was controlled primarily by  
746 bank erosion, and thus by the same variables controlling this process. This finding points to the need to better  
747 understand bank erosion processes and the interactions with vegetation so as to predict or to identify LW  
748 recruitment sources. LW deposition was mostly controlled by channel morphology (i.e., initial channel width and  
749 gradient), and studies like this one are therefore crucial to identify preferential reaches for wood deposition. This  
750 is an important component of the full wood budget, but not the only one. Further efforts in wood budgeting at the  
751 single event temporal scale are key to better understand LW dynamics during floods in mountains rivers.

752

753

#### 754 **Acknowledgments**

755 This study was funded by the Federal Office for the Environment (FOEN) in the framework of the “Large Wood  
756 during the July 2014 Emme Flood Project” (00.0157.PZ/N414-1285) and the “Research Project WoodFlow”  
757 (15.0018.PJ/O192-3154). A part of the work presented here was carried out within the scope of the local,  
758 solution-oriented event analysis of the 24 July 2014 Emme flood event (Lokale, lösungsorientierte  
759 Ereignisanalyse (LLE) Schangnau-Eggiwil) commissioned by the canton of Berne. We thank ARGE GEOTEST  
760 AG and Geo7 AG for the good collaboration. The Forest Division of the Canton of Bern (KAWA) provided the  
761 forest information for the canton of Bern. Massimiliano Zappa helped with the precipitation data handling and  
762 Ramon Stalder and Karl Steiner assisted in the field.

763



764 **References**

- 765 Abernethy, B., Rutherford, I. D. 1998. Where along a river's length will vegetation most effectively stabilise  
766 stream banks? *Geomorphology*, 23(1), 55–75. [https://doi.org/10.1016/S0169-555X\(97\)00089-5](https://doi.org/10.1016/S0169-555X(97)00089-5) Alber, A.,  
767 Piégay, H., 2011. Spatial disaggregation and aggregation procedures for characterizing fluvial features at  
768 the network-scale: Application to the Rhone basin (France). *Geomorphology* 125, 343–360.  
769 <https://doi.org/10.1016/j.geomorph.2010.09.009>
- 770 Andres, N., Badoux, A., Hegg, C., 2015. Unwetterschäden in der Schweiz im Jahre 2014. *Wasser Energie Luft*  
771 107(1), 47-54
- 772 ARGE LLE Schangnau-Eggiwil. 2015. Lokale, lösungsorientierte Ereignisanalyse (LLE) Schangnau-Eggiwil,  
773 Unwetter 24. Juli 2014. Report no. 1414 126.1.
- 774 Arnaud-Fassetta, G., Cossart, E., Fort, M., 2005. Hydro-geomorphic hazards and impact of man-made structures  
775 during the catastrophic flood of June 2000 in the Upper Guil catchment (Queyras, Southern French Alps).  
776 *Geomorphology* 66, 41–67. <https://doi.org/10.1016/j.geomorph.2004.03.014>
- 777 Arnaud-Fassetta G. 2013. Dyke breaching and crevasse-splay sedimentary sequences of the Rhône Delta, France,  
778 caused by extreme river- flood of December 2003. *Geografia Fisica e Dinamica Quaternaria* 36(1): 7–26
- 779 Badoux, A., Andres, N., Turowski, J.M., 2014. Damage costs due to bedload transport processes in Switzerland.  
780 *Nat. Hazards Earth Syst. Sci.* 14, 279–294. <https://doi.org/10.5194/nhess-14-279-2014>
- 781 Badoux, A., Böckli, M., Rickenmann, D., Rickli, C., Ruiz-Villanueva, V., Zurbrügg, S., Stoffel, M., 2015. Large  
782 wood transported during the exceptional flood event of 24 July 2014 in the Emme catchment  
783 (Switzerland). In: *Proceedings of the 3rd International Conference Wood in World Rivers*, Padova, Italy,  
784 July 2015.
- 785 Becker, R. A., Chambers, J. M. and Wilks, A. R. 1988. *The New S Language*. Wadsworth & Brooks/Cole.
- 786 Benda, L.E., Sias, J.C., 2003. A quantitative framework for evaluating the mass balance of in-stream organic  
787 debris. *For. Ecol. Manage.* 172, 1–16. [https://doi.org/10.1016/S0378-1127\(01\)00576-X](https://doi.org/10.1016/S0378-1127(01)00576-X)
- 788 Benito, G., 1997. Energy expenditure and geomorphic work of the cataclysmic Missoula flooding in the  
789 Columbia river Gorge, USA. *Earth Surf. Process. Landforms* 22, 457–472.
- 790 Bezzola, G. R., Hegg, C. (Eds.), 2007. *Ereignisanalyse Hochwasser 2005, Teil 1 – Prozesse, Schäden und erste*  
791 *Einordnung*, Umwelt-Wissen Nr. 0707, Bundesamt für Umwelt BAFU, Bern), Eidg. Forschungsanstalt  
792 WSL, Birmensdorf, Switzerland, 215 pp. (in German).



- 793 Bezzola, G. R., Ruf, W., 2009. Ereignisanalyse Hochwasser August 2007, Umwelt-Wissen Nr. 0927, Bundesamt  
794 für Umwelt BAFU, Bern, Switzerland, 209 pp. (in German).
- 795 Böckli, M., Badoux, A., Rickli, C., Forsting, D., Rickenmann, D., Ruiz-villanueva, V., Zurbrügg, S., Stoffel, M.,  
796 2016. Large wood-related hazards during the extreme flood of 24 July 2014 in the Emme catchment  
797 (Switzerland), in: *Interpraevent 2016*. pp. 190–191.
- 798 Brassel, P., Lischke, H.: Swiss National Forest Inventory: Methods and models of the second assessment. Swiss  
799 Federal Research Institute WSL, Birmensdorf, Switzerland, 336 pp., 2001.
- 800 Bracken, L.J., Turnbull, L., Wainwright, J., Bogaart, P., 2015. Sediment connectivity: a framework for  
801 understanding sediment transfer at multiple scales. *Earth Surf. Process. Landforms* 188, 177–188.  
802 <https://doi.org/10.1002/esp.3635>
- 803 Burkhardt-Holm, P., Scheurer, K., 2007. Application of the weight-of-evidence approach to assess the decline of  
804 brown trout (*Salmo trutta*) in Swiss rivers. *Aquat. Sci.* 69, 51–70. [https://doi.org/10.1007/s00027-006-](https://doi.org/10.1007/s00027-006-0841-6)  
805 [0841-6](https://doi.org/10.1007/s00027-006-0841-6)
- 806 Buraas, E. M., Renshaw, C. E., Magilligan, F. J., Dade, W. B. 2014. Impact of reach geometry on stream channel  
807 sensitivity to extreme floods. *Earth Surface Processes and Landforms*, 1789(April), 1778–1789.  
808 <https://doi.org/10.1002/esp.3562>
- 809 Cenderelli, D.A., Kite, J.S., 1998. Geomorphic effects of large debris flows on channel morphology at North  
810 Fork Mountain, eastern West Virginia, USA. *Earth Surf. Process. Landf.* 23, 1–19.
- 811 Comiti, F., Lucía, A., Rickenmann, D., 2016. Large wood recruitment and transport during large floods: a review.  
812 *Geomorphology* submitted, 23–39. <https://doi.org/10.1016/j.geomorph.2016.06.016>
- 813 Croke, J., Fryirs, K., Thompson, C., 2013. Channel-floodplain connectivity during an extreme flood event:  
814 Implications for sediment erosion, deposition, and delivery. *Earth Surf. Process. Landforms* 38, 1444–  
815 1456. <https://doi.org/10.1002/esp.3430>.
- 816 Daniels, M. D. 2006. Distribution and dynamics of large woody debris and organic matter in a low-energy  
817 meandering stream. *Geomorphology*, 77(3–4), 286–298. <https://doi.org/10.1016/j.geomorph.2006.01.011>
- 818 Dilts, T.E. 2015. Polygon to Centerline Tool for ArcGIS. University of Nevada Reno. Available at:  
819 <http://www.arcgis.com/home/item.html?id=bc642731870740aabf48134f90aa6165>
- 820 Dragulescu A.A. 2014. *xlsx*: Read, write, format Excel 2007 and Excel 97/2000/XP/2003 files. R package  
821 version 0.5.7. <https://CRAN.R-project.org/package=xlsx>



- 822 Ferreira, 2014. Perpendicular Transects (Ferreira). GIS 4 Geomorphology. Available:  
823 <http://gis4geomorphology.com/stream-transects-partial/>
- 824 FOEN (ed.), 2015. Hydrological Yearbook of Switzerland 2014. Federal Office for the Environment, Bern,  
825 Environmental Status no. UZ-1511-E, 36 p.
- 826 FOEN, 2017. Hochwasserwahrscheinlichkeiten (Jahreshochwasser) Emme - Eggiwil, Heidbüel (EDV: 2409).  
827 Federal Office for the Environment, Bern, available at:  
828 [https://www.hydrodaten.admin.ch/lhg/sdi/hq\\_studien/hq\\_statistics/2409hq.pdf](https://www.hydrodaten.admin.ch/lhg/sdi/hq_studien/hq_statistics/2409hq.pdf) (last access: 9 February  
829 2018)
- 830 Fox, J. 2005. The R Commander: A Basic Statistics Graphical User Interface to R. Journal of Statistical  
831 Software, 14(9): 1–42
- 832 Fox, J. 2016. Using the R Commander: A Point-and-Click Interface or R. Boca Raton FL: Chapman and  
833 Hall/CRC Press.
- 834 Fox, J., Bouchet-Valat, M. 2017. Rcmdr: R Commander. R package version 2.3-2.
- 835 Gaume, E., Borga, M., 2008. Post-flood field investigations in upland catchments after major flash floods:  
836 proposal of a methodology and illustrations. J. Flood Risk Manag. 1, 175–189.  
837 <https://doi.org/10.1111/j.1753-318X.2008.00023.x>
- 838 Gaume, E., Livet, M., Desbordes, M., Villeneuve, J.P., 2004. Hydrological analysis of the river Aude, France,  
839 flash flood on 12 and 13 November 1999. J. Hydrol. 286, 135–154.  
840 <https://doi.org/10.1016/j.jhydrol.2003.09.015>
- 841 Gurnell, A.M., 2007. Analogies between mineral sediment and vegetative particle dynamics in fluvial systems.  
842 Geomorphology 89, 9–22. <https://doi.org/10.1016/j.geomorph.2006.07.012>
- 843 Hajdukiewicz, H., Wyżga, B., Mikuś, P., Zawiejska, J., Radecki-Pawlik, A., 2015. Impact of a large flood on  
844 mountain river habitats, channel morphology, and valley infrastructure. Geomorphology.  
845 <https://doi.org/10.1016/j.geomorph.2015.09.003>
- 846 Harrell Jr, F.E. 2016. Hmisc: Harrell Miscellaneous. R package version 4.0-2. [https://CRAN.R-  
847 project.org/package=Hmisc](https://CRAN.R-project.org/package=Hmisc)
- 848 Harvey, A.M., 1986. Geomorphic effects of a 100-year storm in the Howgill Fells, northwest England. Zeitschrift  
849 für Geomorphologie 30, 71–91.



- 850 Harvey, A.M., 2001. Coupling between hillslopes and channels in upland fluvial systems: Implications for  
851 landscape sensitivity, illustrated from the Howgill Fells, northwest England. *Catena* 42, 225–250.  
852 [https://doi.org/10.1016/S0341-8162\(00\)00139-9](https://doi.org/10.1016/S0341-8162(00)00139-9)
- 853 Heritage, G.L., Large, A.R.G., Moon, B.P., Jewitt, G., 2004. Channel hydraulics and geomorphic effects of an  
854 extreme flood event on the Sabie River, South Africa. *Catena* 58, 151–181.
- 855 Hilker, N., Badoux, A., Hegg, C., 2009. The Swiss flood and landslide damage database 1972–2007. *Nat.*  
856 *Hazards Earth Syst. Sci.* 9, 913–925. doi:10.5194/nhess-9-913-2009, 2009.
- 857 Hollis, G.E. 1975. The effect of urbanization on floods of different recurrence interval. *Water Resources*  
858 *Research* 11(3), 431–435.
- 859 Howard, A., Dolan, R., 1981. Geomorphology of the Colorado River in the Grand Canyon. *J. Geol.* 89, 269–298.
- 860 Kevin Wright 2017. corrgram: Plot a Correlogram. R package version 1.12. [https://CRAN.R-](https://CRAN.R-project.org/package=corrgram)  
861 [project.org/package=corrgram](https://CRAN.R-project.org/package=corrgram)
- 862 Krapesch, G., Hauer, C., & Habersack, H. 2011. Scale orientated analysis of river width changes due to extreme  
863 flood hazards. *Natural Hazards and Earth System Sciences*, 11(8), 2137–2147.  
864 <https://doi.org/10.5194/nhess-11-2137-2011>Lapointe, M.F., Secretan, Y., Driscoll, S.N., Bergeron, N.,  
865 Leclerc, M., 1998. Response of the Ha! Ha! River to the flood of July 1996 in the Saguenay Region of  
866 Quebec: large-scale avulsion in a glaciated valley. *Water Resour. Res.* 34 9 , 2383–2392.
- 867 Lehmann, C. 2001. Geschiebestudie hinteres Lauterbrunnental. Unveröffentlicht. Bericht, TBA-OIK-II. Thun
- 868 Lin GW, Chen H, Hovius N, Horng MJ, Dadson S, Meunier P, Lines M. 2008. Effects of earthquake and cyclone  
869 sequencing on landsliding and fluvial sediment transfer in a mountain catchment. *Earth Surf Proc*  
870 *Landforms* 33:1354–1373
- 871 Lucía, a., Comiti, F., Borga, M., Cavalli, M., Marchi, L., 2015. Dynamics of large wood during a flash flood in  
872 two mountain catchments. *Nat. Hazards Earth Syst. Sci. Discuss.* 3, 1643–1680.  
873 <https://doi.org/10.5194/nhessd-3-1643-2015>
- 874 Macklin, M.G., Rumsby, B.T. and Heap, T., 1992. Flood alluviation and entrenchment: Holocene valley floor  
875 development and transformation in the British uplands. *Geological Society of America Bulletin*, 104, 631–  
876 643.
- 877 Magilligan, F.J., Phillips, J.D., James, L.A., Gomez, B., 1998. Geomorphic and Sedimentological Controls on the  
878 Effectiveness of an Extreme Flood. *J. Geol.* 106, 87–96. <https://doi.org/10.1086/516009>



- 879 Marchi L & Dalla Fontana G. 2005. GIS morphometric indicators for the analysis of sediment dynamics in  
880 mountain basins, *Environmental Geology*, 48(2): 218–228.
- 881 Marchi, L., Borga, M., Preciso, E., Sangati, M., Gaume, E., Bain, V., Delrieu, G., Bonnifait, L., Pogačnik, N.,  
882 2009. Comprehensive post-event survey of a flash flood in Western Slovenia: Observation strategy and  
883 lessons learned. *Hydrol. Process.* 23, 3761–3770. <https://doi.org/10.1002/hyp.7542>.
- 884 Marcus, W. A., Marston, R. a, Colvard, C. R., Gray, R. D. 2002. Mapping the spatial and temporal distributions  
885 of woody debris in streams of the Greater Yellowstone Ecosystem, USA. *Geomorphology*, 44(3–4), 323–  
886 335. [https://doi.org/10.1016/S0169-555X\(01\)00181-7](https://doi.org/10.1016/S0169-555X(01)00181-7).
- 887 Mazzorana, B., Hübl, J., Zischg, A., Largiader, A. 2011. Modelling woody material transport and deposition in  
888 alpine rivers. *Natural Hazards*, 56(2), 425–449. <https://doi.org/10.1007/s11069-009-9492-y>
- 889 Mazzorana, B., Ruiz-Villanueva, V., Marchi, L., Cavalli, M., Gems, B., Gschnitzer, T., Valdebenito, G. 2017.  
890 Assessing and mitigating large wood-related hazards in mountain streams: recent approaches. *Journal of*  
891 *Flood Risk Management*. <https://doi.org/10.1111/jfr3.12316>
- 892 Merritts, D., 2011. The effects of variable river flow on human communities. In: Wohl, E.E. (Ed.), *Inland Flood*  
893 *Hazards: Human, Riparian, and Aquatic Communities*. Cambridge Univ. Press, New York, pp. 271–290.
- 894 MeteoSwiss: 24-28 July 2014 Weather situation, available at:  
895 [http://www.meteoswiss.admin.ch/home/climate/past/climate-extremes/extreme-value-analyses/high-](http://www.meteoswiss.admin.ch/home/climate/past/climate-extremes/extreme-value-analyses/high-impact-precipitation-events/24-28-july-2014.html)  
896 [impact-precipitation-events/24-28-july-2014.html](http://www.meteoswiss.admin.ch/home/climate/past/climate-extremes/extreme-value-analyses/high-impact-precipitation-events/24-28-july-2014.html), last access 20 April 2017.
- 897 Milan, D., 2012. Geomorphic impact and system recovery following an extreme flood in an upland stream,  
898 Thinhope Burn, northern England, UK. *Geomorphology* 138, 319–328.
- 899 Miller, A.J., 1990. Flood hydrology and geomorphic effectiveness in the central Appalachians. *Earth Surf.*  
900 *Process. Landf.* 15, 119–134.
- 901 Nardi, L., Rinaldi, M. 2015. Spatio-temporal patterns of channel changes in response to a major flood event: The  
902 case of the Magra River (central-northern Italy). *Earth Surface Processes and Landforms*, 40(3), 326–339.  
903 <https://doi.org/10.1002/esp.3636>
- 904 R Core Team 2017. R: A language and environment for statistical computing. R Foundation for Statistical  
905 Computing, Vienna, Austria. URL <https://www.R-project.org/>.
- 906 Rickenmann, D., Koschni, A., 2010. Sediment loads due to fluvial transport and debris flows during the 2005  
907 flood events in Switzerland. *Hydrol. Process.* 24, 993–1007. <https://doi.org/10.1002/hyp.7536>



- 908 Rickenmann, D., Badoux, A., Hunzinger, L., 2016. Significance of sediment transport processes during piedmont  
909 floods: The 2005 flood events in Switzerland. *Earth Surf. Process. Landforms* 230, 224–230.  
910 <https://doi.org/10.1002/esp.3835>
- 911 Rickli, C., Bucher, H. 2006. Einfluss ufernaher Bestockungen auf das Schwemholzvorkommen in Wildbächen.  
912 Projektbericht Dezember 2006.
- 913 Rickli, C., Böckli, M., Badoux, A., Rickenmann, D., Zurbrügg, S., Ruiz-Villanueva, V., and Stoffel, M 2016.:  
914 Schwemholztransport während des Hochwasserereignisses vom 24. Juli 2014 im Einzugsgebiet der  
915 Emme, *Wasser Energie Luft*, 108(3), 225-231, (in German).
- 916 Rickli, C., Badoux, A., Rickenmann, D., Steeb, N., Waldner, P., 2018. Large wood potential, piece  
917 characteristics, and flood effects in Swiss mountain streams. *Physical Geography*.  
918 <https://doi.org/10.1080/02723646.2018.1456310>.
- 919 Righini, M., Surian, N., Wohl, E., Marchi, L., Comiti, F., Amponsah, W., Borga, M., 2017. Geomorphic response  
920 to an extreme flood in two Mediterranean rivers (northeastern Sardinia, Italy): Analysis of controlling  
921 factors. *Geomorphology* 290, 184–199. <https://doi.org/10.1016/j.geomorph.2017.04.014>.
- 922 Rigon, E., Comiti, F., Lenzi, M. A. 2012. Large wood storage in streams of the Eastern Italian Alps and the  
923 relevance of hillslope processes. *Water Resources Research*, 48(1), W01518.  
924 <https://doi.org/10.1029/2010WR009854>
- 925 Rinaldi, M., Surian, N., Comiti, F., Bussetini, M. 2015. A methodological framework for hydromorphological  
926 assessment, analysis and monitoring (IDRAIM) aimed at promoting integrated river management.  
927 *Geomorphology*, 251(November), 122–136. <https://doi.org/10.1016/j.geomorph.2015.05.010>
- 928 Rinaldi, M., Amponsah, W., Benvenuti, M., Borga, M., Comiti, F., Lucía, A., Marchi, L., Nardi, L., Righini, M.,  
929 Surian, N., 2016. An integrated approach for investigating geomorphic response to extreme events:  
930 methodological framework and application to the October 2011 flood in the Magra River catchment, Italy.  
931 *Earth Surf. Process. Landforms* n/a-n/a. <https://doi.org/10.1002/esp.3902>
- 932 Roux, C., Alber, A., Bertrand, M., Vaudor, L., Piégay, H., 2014. “FluvialCorridor”: A new ArcGIS toolbox  
933 package for multiscale riverscape exploration. *Geomorphology*.  
934 <https://doi.org/10.1016/j.geomorph.2014.04.018>





- 935 Ruiz-Villanueva, V., Díez-Herrero, A., Ballesteros-Canovas, J.A., Bodoque, J.M., 2014. Potential large woody  
936 debris recruitment due to landslides, bank erosion and floods in mountain basins: a quantitative estimation  
937 approach. *River Res. Appl.* 30, 81–97. <https://doi.org/10.1002/rra>
- 938 Ruiz-Villanueva, V., Piégay, H., Gurnell, A. A., Marston, R. A., Stoffel, M. 2016. Recent advances quantifying  
939 the large wood dynamics in river basins: New methods and remaining challenges. *Reviews of Geophysics*,  
940 54(3). <https://doi.org/10.1002/2015RG000514>
- 941 Savi, S., Schneuwly-Bollschweiler, M., Bommer-Dennis, B., Stoffel, M., Schlunegger, F. 2013. Geomorphic  
942 coupling between hillslopes and channels in the Swiss Alps. *Earth Surface Processes and Landforms*,  
943 38(9), 959–969. <https://doi.org/10.1002/esp.3342>.
- 944 Seo, J. Il, Nakamura, F., Akasaka, T., Ichiyanagi, H., Chun, K. W. 2012. Large wood export regulated by the  
945 pattern and intensity of precipitation along a latitudinal gradient in the Japanese archipelago. *Water  
946 Resources Research*, 48(3), n/a-n/a. <https://doi.org/10.1029/2011WR010880>
- 947 Sideris, I. V., Gabella, M., Sassi, M., Germann, U., 2014. The CombiPrecip experience: development and  
948 operation of a real-time radar-raingauge combination scheme in Switzerland. *Int. Symp. Weather Radar  
949 Hydrol.*
- 950 Steeb, N., Rickenmann, D., Badoux, A., Rickli, C., Waldner, P., 2017. Large wood recruitment processes and  
951 transported volumes in Swiss mountain streams during the extreme flood of August 2005. *Geomorphology*  
952 279, 112–127. <https://doi.org/10.1016/j.geomorph.2016.10.011>
- 953 Surian, N., Righini, M., Lucía, A., Nardi, L., Amponsah, W., Benvenuti, M., Viero, A. 2016. Channel response to  
954 extreme floods: Insights on controlling factors from six mountain rivers in northern Apennines, Italy.  
955 *Geomorphology*. <https://doi.org/10.1016/j.geomorph.2016.02.002>.
- 956 Thévenet, A., Citterio, A., Piegay, H. 1998. A new methodology for the assessment of large woody debris  
957 accumulations on highly modified rivers (example of two French piedmont rivers). *Regulated Rivers:  
958 Research & Management*, 14, 467–483. [https://doi.org/10.1002/\(SICI\)1099-1646\(1998110\)14:6<467:  
959 AID-RRR514>3.0.CO;2-X](https://doi.org/10.1002/(SICI)1099-1646(1998110)14:6<467: AID-RRR514>3.0.CO;2-X)
- 960 Thompson C, Croke J., 2013. Geomorphic effects, flood power and channel competence of a catastrophic flood  
961 in confined and unconfined reaches of the upper Lockyer valley, south east Queensland, Australia.  
962 *Geomorphology* 197(1): 156-169. DOI: 10.1016/j.geomorph.2013.05.006



- 963 Wei, T., Simko V. 2017. R package "corrplot": Visualization of a Correlation Matrix (Version 0.84). Available  
964 from <https://github.com/taiyun/corrplot>
- 965 Wells SG, Harvey A. 1987. Sedimentologic and geomorphic variations in storm-generated alluvial fans, Howgill  
966 Fells, northwest England. Geological Society of America Bulletin 98: 182–198.
- 967 Wohl, E., Cenderelli, D. a., Dwire, K. a., Ryan-Burkett, S.E., Young, M.K., Fausch, K.D., 2010. Large in-stream  
968 wood studies: a call for common metrics. Earth Surf. Process. Landforms 625, n/a-n/a.  
969 <https://doi.org/10.1002/esp.1966>
- 970 Wohl, E.E., Greenbaum, N., Schick, A.P., Baker, V.R., 1994. Controls on bedrock channel incision along Nahal  
971 Paran, Israel. Earth Surf. Process. Land. 19, 1–13.
- 972 Wohl, E., 2017. Connectivity in rivers. Prog. Phys. Geogr. 41, 345–362.  
973 <https://doi.org/10.1177/0309133317714972>
- 974 Wyzga, B., 1997. Methods for studying the response of flood flows to channel change. J. Hydrol. 198, 271– 288.
- 975 Zurbrügg, 2015. Hochwasseruntersuchung und Feldstudie zur Quantifizierung des Transports und der  
976 Ablagerung von Schwemmholz während einem extremen Ereignis: Die Überschwemmung vom Juli 2014  
977 in der Emme (Schweiz). Bsc Thesis, University of Bern, Switzerland (in German).
- 978